GENETIC AND BIOLOGICAL CHARACTERIZATION OF ALPHACORONAVIRUS FELINE INFECTIOUS PERITONITIS VIRUS AND GAMMACORONAVIRUS INFECTIOUS BRONCHITIS VIRUS

by

JAMIE EVELYN PHILLIPS

(Under the Direction of MARK W. JACKWOOD)

ABSTRACT

The rapid evolution of RNA viruses makes it difficult to control newly emerging infections. The genomes of RNA viruses evolve by mutations, recombination events, and natural selection. Coronaviruses (CoV) are +ssRNA viruses that are found worldwide, they are highly infectious, and are extremely difficult to control because they have a short generation time and a high mutation rate. They can cause respiratory, enteric, and in certain cases hepatic and neurological diseases, in a wide variety of animals and humans. In the following studies, we found that gamacoronaviruses may have proofreading capabilities similar to other CoVs, which is important for understanding how CoVs can replicate below their error threshold while still maintaining a large genome. In addition, we found that feline coronavirus was surprisingly stable following passage in cell culture, but different selection pressures in vivo may play a role in the pathobiology of that virus. Finally, we found that 10 transmissions of a gammacoronavirus in the natural host resulted in a decreased time to infection but a shorter infectious period. No changes were observed in the S1 gene indicating that mutations may have occurred elsewhere in the viral genome and that age and the maturity of the immune system in the host should be taken into consideration when calculating values for the reproduction ratio R₀. These data will aid in our understanding of the mechanisms behind cross-species transmission, emergence of new CoVs, and viral evolution resulting in drug resistance and vaccine failures.

INDEX WORDS: Coronavirus, genome sequencing, molecular evolution, mutation, selection, subpopulation

GENETIC AND BIOLOGICAL CHARACTERIZATION OF ALPHACORONAVIRUS FELINE INFECTIOUS PERITONITIS VIRUS AND GAMMACORONAVIRUS INFECTIOUS BRONCHITIS VIRUS

by

JAMIE EVELYN PHILLIPS

B.S., Georgia Southern University, 2007

M.S., University of Georgia, 2009

A Dissertation Submitted to the Graduate Faculty of The University of Georgia in Partial Fulfillment of the Requirements for the Degree

DOCTOR OF PHILOSOPHY

ATHENS, GEORGIA

2011

© 2011

Jamie Evelyn Phillips

All Rights Reserved

GENETIC AND BIOLOGICAL CHARACTERIZATION OF ALPHACORONAVIRUS FELINE INFECTIOUS PERITONITIS VIRUS AND GAMMACORONAVIRUS INFECTIOUS BRONCHITIS VIRUS

by

JAMIE EVELYN PHILLIPS

Major Professor: Mark W. Jackwood

Committee: David Stallknecht

Maricarmen Garcia

Matt Sylte Mark Tompkins

Electronic Version Approved:

Maureen Grasso Dean of the Graduate School The University of Georgia December 2011

ACKNOWLEDGEMENTS

I would like to thank my major professor, Mark Jackwood for all his wonderful advice and for always believing in me. I would also like to thank my committee members Maricarmen Garcia, Matt Sylte, Mark Tompkins, and Dave Stallknecht for their expertise and guidance through out my graduate degree. The help and encouragement I received from everyone in the Jackwood lab: Enid McKinley, Debbie Hilt, Sharmi Thor, Hajung Roh, Teneema Kuriakose, Josh Jackwood, Lauren Byrd, and Carey Stewart was invaluable and I can not thank them enough. I would also like to thank the family and friends who have supported me throughout this journey, specifically my husband Gray and my parents, Debbie and Paul Phillips. Finally, all the IDIS students who are too numerous to name, Thank you.

TABLE OF CONTENTS

Pag	e,
ACKNOWLEDGEMENTS i	V
LIST OF TABLESv	/i
LIST OF FIGURESvi	ii
CHAPTER	
1 Introduction	1
2 Literature Review	3
3 Comparative Analysis of Nonstructural Protein 14 in the Replication	
Transcription Complex of Infectious Bronchitis Virus2	8
4 Molecular Characterization of Feline Infectious Peritonitis Virus:	
Comparative Sequence Analysis of full-length genome of FIPV at Different	
Tissue Passage levels	7
5 Transmission Dynamics of Gammacoronavirus Infectious Bronchitis Virus .5	9
6 Conclusions	9

LIST OF TABLES

Page
Table 3.1: Viruses examined for the exoribonuclease domain with corresponding
accession numbers. 34
Table 4.1: Nonstructural proteins in ORF 1a and 1ab locations and changes that occurred
between passages of the virus in Feline Coronavirus 79-1146, pass 8, and pass 50
50
Table 4.2: Location of open reading frame, size of protein, and differences that occurred
in passages of the virus in Feline Coronavirus 79-1146, pass 8, and passs5051
Table 4.3: List of Coronavirus isolates and strains included in the sequence and
phylogenetic analysis of FIPV study52

LIST OF FIGURES

	Page
Figure 3.1: Schematic diagram of nonstructural protein 14	35
Figure 3.2: Phylogenetic tree of nonstructural protein 14	36
Figure 4.1: Phylogenetic tree of all available full length FCoV genomes	54
Figure 4.2: Simplot analysis of Alphacoronaviruses	55
Figure 4.3: Growth Curve Analysis of FIPV WSU79-1146 isolates at different tissue	<u>,</u>
passage levels	56
Figure 4.4: Protein 3C alignment	57
Figure 4.5: Potential N-glycosylation sites in the spike protein of FCoV/FIPVWSU7	9-
1146 p50	58
Figure 5.1: Scatter plot of the CT values from tracheal vs. choanul swabs	69
Figure 5.2: Diagram of the natural transmission study	70
Figure 5.3: Lag Period - The average time from infection to detection of the virus in	the
birds in the natural transmission study	71
Figure 5.4: Infectious Period -The time (hrs.) the infected birds were identified as	
positive for virus isolation.	72
Figure 5.5: Alignment of S1 of Arkansas DPI: inoculum, virus isolated from B-4	
(Transmission 3), and B-21 (Transmission 10).	73

CHAPTER 1

INTRODUCTION

Coronaviruses

Viruses in the order Nidovirales, family Coronaviridae, *genus Coronaviruses* are important pathogens of many species of animals, as well as humans. Coronaviruses (CoV) are spherical enveloped particles that have club shaped spikes. The envelope is formed during budding from an intracellular membrane. The virions range in size from 120-160nm in diameter. The virion contains a single stranded positive sense RNA genome that is approximately 27 to 32 kb in length. Coronaviruses are divided into three groups based on genetic characteristics (alpha, beta, and gamma) and then further subdivided based on increased genomic similarity and serology. In this work, we focused on two important animal coronaviruses, one that infects domestic cats (feline coronavirus) and one that infects chickens (infectious bronchitis virus).

Feline coronavirus (FCoV), an alphacoronavirus, has two pathotypes. The most common pathotype causes a transient asymptomatic infection or a mild self-limiting gastrointestinal disease, and its etiology is a feline enteric coronavirus (FECV). In contrast, a fatal, multisystemic, immune-mediated disease can occur, in a small number of cats, predominantly under the age of two years, which is caused by Feline Infectious Peritonitis virus (FIPV). There are two hypotheses about the origin of FIPV. The first is the mutational hypothesis, which states FECV infected animals develop the fatal form of the disease via genetic mutations that arise during FECV replication. The second hypothesis is that there are two circulating similar viruses that cause different diseases in cats. Determining the capacity of the viral genome to change during adaptation to the host is important to understanding viral evolution and will shed light on these hypotheses.

Classified as a gammacoronavirus, Infectious Bronchitis Virus (IBV), causes an upper respiratory tract infection in chickens. The virus replicates in the sinuses and trachea, as well as numerous other epithelial tissues. All ages of chickens are susceptible to IBV, but the disease is most severe in chicks less than 2 weeks old. Mortality varies depending on the virus serotype, type of bird, age, immunity, environmental stressors, and secondary bacterial infections. Infectious bronchitis virus is highly infectious, and morbidity can be as high as 100% when secondary bacterial pathogens are present. Infectious Bronchitis Virus is difficult to control because new serotypes of the virus continue to emerge in the field. This is thought to be the result of changes in spike accumulating as the virus is transmitted in the flock. Understanding the evolutionary dynamics for IBV is important for controlling the disease, and is a first step to understanding mechanisms that enable the shift in dominant subtypes and the emergence of new serotypes.

Objective 1- Perform comparative sequence analysis on the exoribonuclease domain in nonstructural protein 14, which is thought to be involved in proofreading capabilities in alpha-, beta- and gamma- coronaviruses to identify if, it is conserved in all of the groups.

Objective 2-Sequence the full-length genome of FCoV/FIPV/FCoV WSU 79-1146 at tissue passage levels 1, 8 and 50 to identify genetic changes associated with passage, and examine the growth kinetics of the virus at each passage level to determine if adaptation of the virus has occurred.

Objective 3-Identify the length of the latent and infectious periods, the onset of clinical signs, and the amount of viral shedding that occurs with IBV infection by conducting a natural chain of transmission experiment in chickens.

Objective 4-Sequence the spike glycoprotein gene of IBV isolates (initial inoculum, transmission event 3, and transmission event 10) from the natural chain of transmission experiment (objective 3) to investigate changes in the spike glycoprotein resulting from the virus being naturally transmitted from host to host.

CHAPTER 2

LITERATURE REVIEW

History

In 1930, IBV was identified in poultry. Nearly a decade later, two other CoVs were also identified; Transmissible Gastroenteritis Virus (TGV) and Mouse Hepatitis Virus (MHV). During this time, virologist identified CoVs by their characteristic spike protein using the electron microscope. Subsequently, other CoVs have been identified. Severe Acute Respiratory Syndrome Coronavirus (SARS-CoV), responsible for the 2003 epidemic, led to an explosion of work in this family of viruses. Before the outbreak of SARS-CoV, there were only ten CoVs where the sequence of the complete genomes were known; they are as follows:

(1) Human Coroanvirus 229E (HCoV-229E); (2) Human Coronavirus OC43 (HCoV-OC43); (3) MHV; (4) TGEV; (5) Bovine Coronavirus (BCoV); (6) Porcine Hemagglutinating Encephalomyelitis Virus (PHEV); (7) Porcine Epidemic Diarrhea Virus (PEDV); (8) Porcine Respiratory Coronavirus (PRCV); (9) FCoV; (10) IBV (71, 93).

Alphacoronaviruses are subdivided into group 1a and 1b, due to phylogenetic clustering. No additional group specific characterizations such as gene contents, transcription regulatory sequences (TRS) or other unique genomic features for alpha-CoVs have been described. The two subgroups of alpha-CoVs (1a and 1b) share some similarities, but they are not genetically close enough to be grouped together (93). For example, the CoV Study Group of the International Committee on Taxonomy of Viruses (ICTV) recently proposed naming group 1a CoV "Geselavirus", meaning "Gene Seven Last," but some of group 1b (such as BatCoV-HKU8) also contain this unique ORF downstream of the nucleocapsid (N) protein (93).

Betacoronaviruses were originally grouped together because they possessed a haemagglutinin esterase (HE) protein and two papain-like proteases (PLP1 and PLP2). Since the addition of SARS-CoV to this group, which does not have an HE protein, these parameters are no longer valid. The SARS-CoV was grouped as a betacoronavirus based on 19 out of the 20 conserved cysteine residues in the amino-terminal domain of the S protein (93). Based on full-length genome sequencing, SARS-CoV has been identified as an early split-off from the beta CoV lineage, and was places in a separate subgroup designated 2b (81).

In 2005, a SARS-like virus was identified from four different species of horseshoe bats in Hong Kong and in China. These viruses had greater than 95% amino acid similarities in the nonstructural protein (nsp) 12, nsp 13 and the N gene (93). In 2006, two additional subgroups, 2c and 2d were proposed for the beta CoVs. The subgroups were based on genomic features, which included two PLPs for 2a, while subgroups 2b, 2c, and 2d only encode one PLP. Subgroup 2b contains several small open reading frames (ORF) between the M and N genes while group 2d contains small ORFs downstream of the N gene (93). As more full-length genomes are sequenced, it is likely that the manner in which these CoVs are grouped will continue to change.

Since the discovery of IBV in 1937, gammacoronaviruses were only isolated from avian hosts. This changed in 2008 when an IBV-like virus, SW1, which was isolated from the liver of a dead Beluga whale (*Delphinapterus leucas*) (56). The viral genome of SW1 was sequenced and found to be the largest CoV RNA genome, with an additional 4,105 nucleotides between the M and N proteins. Several other gamma CoVs were recently identified from three different families of birds: the bulbuls (*Pycnonotus spp.*), thrushes (*Turdus spp.*), and munias (*Lonchura spp.*) (94). A novel mammal CoV, isolated from the Asian leopard cat (*Prionailurus bengalensis*), grouped with the avian CoVs, but this grouping was not based on full-length genome phylogenetic analysis (24).

Viral RNA and Proteins

The 5' end of the CoV viral genome has a leader sequence consisting of 65 to 98 nucleotides. This same leader sequence is also found on the 5' end of all subgenomic

mRNA that are made during virus replication. Downstream of the leader sequence is an untranslated region (UTR) that is approximately 200 to 400 nucleotides long. Another UTR is located at the 3' end of the genome, followed by a poly (A) sequence.

Transcription occurs through a leader primed RNA synthesis that results in a set of six 3' co-terminal subgenomic mRNA molecules. Four structural proteins: the Spike (S), Envelope (E), Membrane (M), and the Nucleocapsid (N), along with the viral RNA, make up the virion. In addition to these four structural proteins, betacoronavirues express a HE protein. All CoVs have group specific proteins that are interspersed between the structural proteins. Functions for most of these group specific proteins are unknown.

Translation occurs via the 5' prime two-thirds of the genome. This area of the genome is made up of two polyproteins, (denoted 1a and 1a/b). The latter is translated through a minus one frame-shift translation mechanism. These polyproteins are post-translationally cleaved into 15 or 16 nonstructural proteins (nsp) to make the replication transcription complex (RTC). The nsp 5, which contains the main protease (MPro), cleaves 11 out of the 15 nsps, whereas nsps 2, 3, and 4 are cleaved by the papain like proteases PLP(s), which are located in nsp 3. Most CoVs express two PLPS, but in SARS-CoV and IBV, only one has proven to be functional. As a result, PLP2 cleaves at both PLP1 and PLP2 sites in these viruses with only one functioning PLP (96).

Nonstructural proteins 2, 4, and 6 contain hydrophobic residues predicted to be participants in anchoring the replication system to the Golgi aparatus. Nonstructural proteins 7-10 are reported to have RNA binding activity (8). Nonstructural protein 9 forms a stable homodimer and plays a role in viral replication (8). Nonstructural protein 11/12 is the RNA dependent RNA polymerase, and nsp 13 is a predicted RNA helicase. Nonstructural protein 14 is an exoribonuclease, and it was shown that the fidelity of the viral polymerase was decreased in MHV nsp 14 mutants (27). Nonstructural protein 15 is an endoribonuclease, and nsp 16 is a methyltransferase (96).

The S protein is a glycosylated protein and forms large spikes on the surface of the virion. It mediates attachment to the host cell, is responsible for fusion of the host cell membrane and viral envelope, and contains neutralizing epitopes. In beta- and gamma-CoV, the S protein is post-translationally cleaved into two subunits designated S1 and S2. The S1, a class I fusion protein, forms the outer globular portions of the spike, and is

highly variable among different types of CoV. The S2 subunit forms the stalk region, is acylated, and contains two heptad repeat motifs.

The S protein was originally thought to be the sole determinant of pathogenicity. While this remains true for some CoVs, it is not the case with IBV. The spike glycoprotein gene from a pathogenic IBV isolate (Massachusetts) was inserted into an attenuated strain of IBV, and the resulting recombinant virus was immunogenic but remained an attenuated phenotype (42). In another study, the replicase genes, which encode two polyproteins in an attenuated virus, were cloned into a virulent virus and the resulting virus was attenuated (13). Based on these two studies, it appears that the replicase proteins 1a and 1a/b play a role in the virulence of IBV while in other CoVs the spike is still the sole determinate of pathogenicity.

The HE protein is a beta CoV specific protein, which protrudes from the surface of the virion, and plays a role in binding and entry of beta CoVs into the host cells. In BCoV, the HE protein is approximately 424 amino acids, and has an estimated molecular weight of 62 to 65 kDa (72). The HE protein is a membrane bound homodimer that is linked by disulfide bonds (41, 72).

The E protein plays a role in viral assembly, and has been identified as a type II integral membrane protein (52). The C-terminal region is extended in the cytoplasm, where as the N- terminus is hydrophobic and lies within the membrane (53). Virus-like particles (VLPs) can be formed by expressing the E and the M proteins together in cells (17). In another study, it was reported that the expression of MHV E protein was sufficient for VLP formation of MHV (52). The E protein is approximately 9 to 12 KDa in size and is present in small quantities in the virion. The IBV E protein is found in abundant amounts at late time points post-infection and in the Golgi complex (52). Therefore, in addition to virus assembly, the E protein might have other functions. One such function is induction of apoptosis in infected cells, which has been shown to occur for the MHV E protein (3).

The M protein is a triple membrane spanning protein. It is also the most abundant envelope protein, and is highly glycosylated. The result, is a virion with a hydrophilic cover on its surface (21). The M protein functions with the E protein to allow virus assembly. Furthermore, the M protein, specifically in its C-term region, has been shown

to interact with the viral N protein. Alpha and gamma CoVs encode M proteins that are N-linked glycosylated, while beta CoVs are O linked glycosylated. The glycosylation sites are not required for virus assembly; and it is thought that they serve a role in virus-host interactions (21). The role of glycosylation of the M protein in MHV and unglycosylated M proteins were poor interferon inducers (21). It was also studied that, N-linked glycosylation sites induced much higher levels of type I interferon than those with O –linked glycosylation sites.

The N protein is a phosphoprotein of 50 to 60 kD, and is relatively conserved among the various CoV groups. It is one of the most abundant proteins found in infected cells and it serves multiple functions. Its main functions are to form a complex with the viral genome, resulting in a ribonucleocapsid structure (19), and associates with the M protein to form the viral core (76). Many CoV (IBV, MHV, and TGeV), N proteins, have been identified as being phosphorylated (15). In one study, a phosphorylated N protein from IBV bound to viral RNA with a higher affinity than a nonphosphorylated N protein (15).

One conserved region in the N protein is the RNA binding domain, which is located in the middle of the protein and has been identified to bind to the leader sequence of viral RNA (15). More recently, Hurst *et al.* replaced the MHV N gene with a closely related Bovine CoV (BCoV) N gene (45). The viral mutant was defective despite the fact that the regions of the N protein (previously shown to interact with RNA) and the M protein are interchangeable for MHV and BCoV. The area of the N protein that was thought to be responsible for making the mutant defective was the serine-arginine-rich (SR) domain. These amino acids reverted to wild type following replication of the virus in vitro. Furthermore, they found that mutations were also introduced in the nsp 3 gene at the amino terminus coding region that reverted the functionality back to wild type. Using the N protein from SARS-CoV, they were able to further confirm the interaction between N and nsp 3 (45). These data, and data from previous studies, indicate that the N protein tethers the genomic RNA to the newly translated replicase via nsp 3, and is a prerequisite for the formation of the initiation complex at the 3' end of the genome (45). The N protein has also been shown to be an type I interferon antagonist (95).

Cellular receptors

The S glycoprotein confers host specificity in CoVs. Studies have previously shown that subtle changes in the S gene are sufficient to affect species tropism and virulence of a CoV (10). Some alpha CoVs (CCoV, FIPV, HCoV-229E, and TGeV) bind to aminopeptidase-N (APN/CD13); a family of zinc-binding metalloproteinases found in epithelium and fibroblast cells located in the small intestine, renal epithelium, central nervous system, and on cells of monocyte and granulocyte lineages (23). However, FCoVs type I do not bind to the APN receptor. Rather, they use dendritic cell specific (DC) intracellular adhesion molecule 3 grabbing non-integrin (DC-SIGN) for entry into Crandell feline kidney cells (CrFK) (88). Mouse Hepatitis Virus (MHV), a beta CoV, has been shown to use the Carcinoembryonic antigen cell adhesion molecule, which is classified as an Ig superfamily (CeaCam1) (26). In contrast, Bovine CoV, also a beta CoV, uses 9-O-acetylated sialic acid as a receptor (78). SARS CoV and HCoV-NL63 have been shown to use ACE2 (33). Gamma CoV(s) are thought to use sialic acid as a correceptor but the exact receptor is unknown (91).

Adaptability of Coronaviruses

Coronaviruses infect a variety of animals including humans and cause different diseases. Evidence of zoonotic transmission and change in host or tissue tropism have been identified, which reflect their ability to easily adapt to new environments. This was clearly demonstrated in 2002-2003 when the SARS-CoV infected humans after first being transmitted from bats, to a palm civet (34).

Most of the identified CoV(s) are species, organ, and even tissue specific; but this specificity can change with only minor genetic differences. For example, FECV and FIPV, are serologically and morphologically identical however, FIPV is able to infect or replicate in macrophages more efficiently than FECV, where it causes a systemic fatal. Another example is the closely related JMK and Gray strains of IBV. Infectious Bronchitis Virus, strain JMK causes an upper respiratory disease in chickens and Gray causes a nephropathogenic disease but the two viruses are 98% related at the nucleotide

level (86). In addition, porcine epidemic diarrhea virus, which infects pigs, emerged in the 1970's from an unknown host suggesting that host species transmission occurs in CoVs (71). Another example of a change in host specificity is the closely related Human CoV OC43, which is thought to be derived from bovine CoV (89). In 1995, an unidentified CoV was isolated from the enteric tract of turkeys in North Carolina (35). This virus was later characterized, and the genome was similar to IBV with the exception of the S glycoprotein. These data suggest that a recombination event occurred, leading to the emergence of Turkey CoV (46). Coronaviruses have the ability to: adapt to a new host, evade the immune system and change cellular tropism. The ability of CoV's to do this is a result of three major factors; first the infidelity of the CoV RNA-dependent RNA polymerase (even though some proof reading capabilities may exist) the mutation rate can be calculated in the order of 1 per 1,000 to 10,000 nucleotides synthesized (93). Second, CoVs replicate by a "copy choice mechanism" that leads to homologous recombination and third, the CoV genomes are the largest of all known RNA viruses, giving them extra plasticity (93). This ability to adapt was shown for the MHV E deleted mutant, which duplicated a portion of its M gene to replace the function of the E protein (50).

Viruses adapt to a new host by a process referred to as natural selection. This process is also thought to reduce deleterious mutations and select for mutants that have an advantage in a particular host. When a gene is highly divergent, such as the S protein, there are two accepted explanations. One explanation is that the gene is free to mutate because it serves no function. Another explanation is that the gene is critical for survival and diverges due to positive selection, as a result of natural selection (85).

Recombination

Recombination is thought to occur at a high frequency for CoVs (5, 40). One study estimated the recombination frequency of MHV at 1% per 1,300 nucleotides, or approximately 25% for the entire genome (5). Recombination allows for the rapid exchange of genetic material that may enable the virus to quickly adapt to new

environments. The occurrence of recombination has been identified in tissue culture, in experimentally infected animals, in embryonated eggs, and in the field (40).

The replication process of CoVs, uses a discontinuous transcription mechanism that adds a mRNA leader sequence, usually derived in-trans, from a different RNA molecule. This requires the polymerase to dissociate from the template and reattach to a new molecule during negative and positive strand RNA synthesis (40). This method of replication is referred to as the "copy choice" mechanism. The name implies that the RNA dependent RNA polymerase (RdRp), along with the nascent cRNA, dissociate or "jump" from the original template and re-associate with another template at a nearly identical site where RNA synthesis continues (40). If two different strains of CoV infect the same cell, recombination can occur from the RdRp, re-associating with the template of the other strain and producing a chimeric viral genome.

Feline Coronaviruses

The FCoVs are alphacoronaviruses that are subdivided into type I and II. Type I FCoVs are considered the "wholly" feline virus, where as type II has been identified as recombinants between Canine Coronavirus (CCoV) and FCoV. Multiple recombination events are believed to have taken place between FCoV and CCoV. For example, a recombination event occurred and inserted the S glycoprotein and the 3' adjacent genes from CCoV into the FCoV genome (40). Other phylogenetic studies indicate that CCoV, FCoV, and Porcine CoV have undergone recombination events, suggesting that they were present in the same host at some time (51). In deed, it has been shown experimentally that CCoV is able to use the feline aminopeptidase (fAPN) glycoprotein as a cellular receptor and that cats can be infected with CCoV (6, 77).

The ICTV believed that TGEV, FCoV type II, and CCoV should not be considered separate viruses because of the close genetic relatedness. Rather they should be identified as a single virus type having a broad host range (22). The current geographical distribution of FCoV indicates that Europe, Japan, and the US have a high incidence of Type I FCoV (25), whereas type II makes up more than 30% of isolates in Japan (66).

There are two variants of FCoV, which are morphologically and antigenically indistinguishable, but upon inoculation of animals these variants present two different biological diseases (67). One, feline enteric virus (FECV), is typically asymptomatic and may produce mild diarrhea that is transient, whereas the other causes a systemic lethal infection and is designated feline infectious peritonitis virus (FIPV).

Epizootiology of Feline Infectious Peritonitis Virus

Feline Infectious Peritonitis Virus is mainly described as a disease of cats but it has also been reported in the African lion, the Mountain Lion, the Leopard, Cheetah, Jaguar, Lynx, Serval, Caracal, European Wild Cat, Sand Cat, and Pallas Cat (66). A separate virus, causing an almost identical disease in ferrets (66). Found all over the world, the epidemiology of FIPV is closely linked to FECV. One third of all older cats, and 90% of kittens and juveniles that were presented to an animal shelter in Sacramento, CA USA, were shedding FCoV at the time of entry (68).

History of Feline Infectious Peritonitis

Feline Infectious Peritonitis was first documented in the late 1950s by necropsy records at the Angell Memorial Animal Hospital, Boston MA. From this point on, there was a steady increase in the incidence of the disease and now it is one of the leading causes of death in young cats in shelters (66). Holzworth officially described FIPV in 1963, but it was not until 1966 when Wolfe and Griesmer showed that a viral agent was the cause of FIP (43, 92). In 1972, Montali and Strandberg reported that the virus causes two different forms of the disease identified as wet and dry forms. In 1978, the antigenic relationship of FIPV to canine, porcine, and human CoVs was elucidated (69). Although both the FIPV and the FECV were morphologically and antigenically similar, it became apparent that they were two distinct entities. Feline infectious peritonitis virus and FECV can currently only be distinguished by the clinical disease they cause in cats (66).

Diagnosis of Feline Infectious Peritonitis Virus

Feline Infectious Peritonitis Virus causes two different types of disease; a wet form and a dry form (66). Both forms can occur together. The wet form of the disease, sometimes referred to as the effusive form, is caused by the accumulation of fluid in the peritoneal cavity or chest. The fluid in the peritoneal cavity is caused by immune complex vasculitis resulting in a distended abdomen (80). In cats that have some cell-mediated immunity the dry form (non-effusive form) can be identified by a lack of appetite, fever, jaundice, diarrhea, eye lesions in the iris, and weight loss (80). While both forms of the disease are fatal, the wet form is diagnosed more frequently; approximately 60-70% of all FIPV cases are the wet form. However, the dry FIP form may become effusive in the later stages of the disease, as the cat's immune system collapsese from a decrease in CD4+ cells (64). Because these are symptoms that resemble other infections, the diagnosis of FIPV is challenging and is usually based on several factors, serology, tissue biopsies, and PCR (9). Ultrasonography and radiographs are other means to diagnose the accumulation of fluid in the abdomen (74).

One consistent laboratory finding in FIP cats is an increase in serum protein concentration, specifically hyperglobulin concentrations (82). This is found in 50% of cats with the dry form of the disease and about 70% of cats with the wet form of the disease. The increase in serum protein leads to a decreased albumin-to-globulin (A:G) ratio and an A:G ratio less than 0.4 can be an indicator of FIP (37).

The measurements of antibodies are not used specifically for FIPV diagnostic purposes but more for the absence of detection of FCoV infection because a high percentage of cats have antibodies against FCoV. The testing of antibodies is more useful for differentiating FCoV free cats for catteries (74). There is a commercial kit available for the detection of FCoV antibodies it is ImmunoComb FCoV Antibody Test Kit (Biogal, Israel) (1).

Transmission of Feline Coronavirus

Epidemiological studies indicate some FCoVs cause chronic enteric infections that are asymptomatic and these may serve as the carriers that spread the infection to susceptible kittens via a fecal oral route (39). The majority of cats that live in multi-cat environments shed FCoV at any given time. Most of the infections are cyclic; the cats shed the virus, recover, and then are re-infected (28). There are three essential factors for the continued transmission of FIPV (65):

- 1. A reservoir of infected animals that are shedding virus
- 2. A continuous source of susceptible animals
- 3. Unfavorable environmental conditions that enable fecal-oral transmission

There is evidence of chronic infections; the virus has been shown to persist in the intestine and other organs of healthy cats. These carriers may excrete virus for months or even years (7). Looking at persistence and transmission of FCoVs over a seven year period, one study characterized the FCoVs that were shed by domestic cats. Using RT-PCR, the 3' end of the S gene was amplified, enabling the researcher to distinguish between type I and type II FCoVs (2). The majority of cats were infected with a single strain of the virus, but some were infected with more than one strain. Persistent or transient infections did not appear to be linked to different virus strains. The factors that determine if FCoV establishes persistent infections or ephemeral appear to be based on the host response to the virus and not the type of FCoV (2).

Infection of Feline Infectious Peritonitis Virus

Feline Infectious Peritonitis Virus mainly causes disease in young cats. Death occurs shortly after weaning and appears to peak at six to eighteen months (7, 69). Mortality usually decreases after eighteen months and relatively few cases occur after three to five years of age. Over seventy-five percent of FIP cases that occur in the USA are in catteries or multi-cat households (65). The overall mortality rate for household cats, where one or two older cats are present is 1:5,000, while densely housed groups of

cats have a 5% mortality rate for FIP (65). There is a higher incidence of FIP in pure breed cats and cheetahs, which may indicate that the cats that develop FIP are genetically predisposed (7). In addition, to age and breed, the sex of the cat can also influence the disease. Several studies have shown that males have a higher incidence of FIP than females (7, 73).

Immune response to Feline Infectious Peritonitis Virus

Feline Infectious Peritonitis Virus, causes a highly lethal disease that is characterized by acute lymphopenia, fever, weight loss, and depletion of CD4+ and CD8+ T cells (20). Experimental inoculation with the highly virulent strain 79-1146 causes mortality in 20 to 30 hours post infection (36). Clinical FIP does not occur until the virus crosses the mucosal barrier and spreads via infected macrophages and monocytes (32). This occurs when the virus is ingested by a macrophage, often in the mesenteric lymph node and replicates in the cytoplasm of the macrophage causing the release of new virions (65). The ability to replicate in the macrophage is a major difference between the FECV and FIPV (83). Once FIPV starts to replicate in the macrophage it ultimately becomes systemic spreading to other tissues and organs. The characteristic lesions from FIP are a result of the macrophages congregating around small venules in the tissues causing the classical vascular inflammation (65).

In the late stages of FIP it has been shown that non-neutralizing antibodies promote disease by enhancement of virus infection in mononuclear phagocytes or by the formation of immune complexes, activation of complement, and secondary vascular disturbances (90). In addition, it has been shown that administration of antibody to cats prior to FIP infection actually exacerbates the disease (84).

Type I versus Type II FCoV in Cell Culture

The majority of research with FCoV has used Type II FCoV because these viruses grow more readily in cell culture. However, the ability to propagate FCoV in cell culture does not correlate with virulence in vivo (57). Type I FCoV (UCD1, UCD2, UCD3,

UCD4, TN-406, NW1, Yayoi, KU-2, Dahlberg, FECV UCD) show no or very little signs of replication in cell culture. While, group II (FIPV 79-1146, NOR15 (DF-2), Cornell-1, FECV 79-1683) induce cytopathic effect in cell culture (7).

Infectious Bronchitis Virus

Infectious bronchitis virus, a gammacoronavirus, causes a highly contagious disease in chickens. The economic impact can be significant because this virus is difficult to control due to its high transmissibility and the constant emergence of new serotypes. While mortality is usually low in uncomplicated infections, it can be severe in young chickens, or when the disease is complicated by secondary pathogens. In broilers a reduction in weight gain, tracheal rales, coughing, and sneezing are characteristic clinical signs of IBV infection. In layers, a decline in egg production and egg quality can result from infection with IBV. In addition to causing respiratory stress in the birds, some strains have been shown to cause nephritis.

The distribution of the virus is worldwide. In the United States, several serotypes have been identified include: Massachusetts, Connecticut, Delaware, Georgia 98, Arkansas-DPI, JMK, Florida, and Gray. Massachusetts-like viruses have been isolated in Europe as well as Asia since the 1940's. Numerous other serotypes have been identified all over the world from Africa to China, however, little cross protection is observed between the different serotypes.

Transmission of IBV

Infectious Bronchitis Virus spreads rapidly through flocks and has a short incubation period, with birds developing clinical signs as early as 24 to 48 hours following experimental infection (12). The incubation time for IBV can be as short as 18 hours for intratracheal inoculation and up to 36 hours for ocular inoculation depending on viral dose (12). The virus can be isolated from the trachea, lungs, kidney, cecal tonsil, and the bursa of Fabricius for up to seven days after the initial infection. One study indicated that IBV can be shed periodically for up to 72 days from chickens (61). In addition, it

has been shown that the Arkansas vaccine strain can persist in commercial broilers for an extended amount of time (47).

Vaccination for Infectious Bronchitis Virus

The most common method of control for IBV is vaccination. This method of control was started in the 1950s with live attenuated vaccines, and inactivated viruses were developed for vaccine usage later in the 1970s (11). Attenuated live vaccines can be administered by eye drop or intranasally. These routes of vaccination give the best response, but they are labor intensive. Thus, mass application methods are used in poultry houses such as coarse spray, aerosol, and drinking water.

In broilers the initial inoculum for an attenuated live vaccine is given at one day of age and then followed by a boost. These attenuated live vaccines are serially passaged in embryonating chicken eggs(14). Due to the blind passaging, the attenuation of the vaccines varies between serotypes. It has been demonstrated that some vaccines can revert back to virulence after being back passaged in chickens (44). The mechanism of attenuation is unknown in these blind passages but this could be corrected by genetically manipulating the IBV genome. This type of vaccine would also enable the swapping of the spike protein for new serotypes (14).

Several molecular subunit vaccines have been created for IBV using Pox and HVT vectors but only partial protection was achieved using these. DNA vaccines have been created that were affective but the problem with these lie in the administration for mass vaccination, which is needed in the poultry industry (75).

Vaccine efficacy testing has changed over the years. In the 1970's, proof of seroconversion was considered the gold standard. Although this method is still used for inactivated vaccines, live vaccines are evaluated by protection from challenge at 3 to 4 weeks post vaccination. The criteria used to assess protection in the USA is failure to recover challenge virus from 90% of the vaccinated bird at 5 days post-challenge (87).

Immune Response to Infectious Bronchitis Virus

Infectious Bronchitis Virus initially infects ciliated columnar epithelial cells in the upper respiratory tract. This virus replicates in ciliated epithelium and mucous-secreting cells (12). The virus reaches maximum titer in the trachea within three days and can remain at this level for two to five days (12). Replication in the upper-respiratory tract is followed by viremia resulting in the dissemination of the virus to other tissues (75). Coronaviruses often disseminate to the kidneys, oviduct, testes, jejunum, Harderian gland, and bursa of Fabricus (12). The susceptibility to the disease varies due to several factors including, but are not limited to breed, age, nutrition, environment, and secondary bacterial infections (75).

Both the cell mediated and humoral immune responses play an important role in protection against IBV infection and in recovery from the disease. However, much of what is known about the immune response to IBV is the humoral response due to its protective function. Chickens develop a humoral immune response to IBV initially producing Immunoglobulin M (IgM), which is transitory and reaches the highest titer at around eight days post infection (58). Anti-IBV IgG can be detected following a second exposure to IBV as early as four days post infection and then reaches a peak around 21 days (58). Homologous antibodies were shown to protect the trachea epithelium following a secondary challenge (74). Several studies have looked at the importance of B-cells using depletion experiments, all of which led to an increase in the severity of the disease (74). However, no mortality was seen in the B-cell depleted birds. Around 14 days post infection IgA can be found in the mucosal lining of the respiratory track, and in tracheal washes for up to 44 days (38). Specific IgA against IBV has also been found in the lachrymal fluids of chickens that are resistant to IBV (16).

Passive immunity due to maternally-derived antibodies (MDA) can dampen the efficacy of a vaccine if the vaccine is homologous to the maternal antibodies in the yolk sac (14). Despite this, the process of vaccinating one-day-old commercial chickens is routine. Chicks have >95% protection against challenge at one day of age but <30% at seven days of age (59).

The cell mediated immune response has been shown to be critical in the clearance of IBV (79). Initially, there is an increase in cytotoxic T-cells (CTL), which has been shown to inversely correlate with a decrease in viral load and clinical signs (77). The protective cellular response is CD8+/CD4-, and peaks at ten days post infection and starts to decline as the IgG humoral immune response increases. The adoptive transfer of IBV specific CD8+ memory T cells that were collected from birds 3-6 weeks post infection were protective for chicks infected with IBV (70).

Identification of Subpopulations in Infectious Bronchitis Virus

To date, several studies have clearly identified viral subpopulations in the field strains and in vaccine vials of IBV (31, 55). The existence of subpopulations in IBV, was demonstrated when McKinley *et al.* identified subpopulations in the egg adapted modified live vaccines (55). To identify if selection was playing a role in the presence of subpopulations, the vaccine virus was reisolated from vaccinated chickens and subsequently back passaged in embryonated eggs. The sequence of the spike glycoprotein was compared, and demonstrated that different subpopulations were selected *in vivo* and *in vitro* (55). The observation of subpopulations was further studied *in vivo* by identifying tissue specific viral subpopulations in the Arkansas strain of IBV (30).

Genetic Variants of Infectious Bronchitis Virus

Infectious bronchitis virus can rapidly mutate resulting in different variants and genetic types of the virus. This was first observed with the IBV Arkansas serotype in the Delmarva Peninsula during 1993-1997. Despite vaccination against the Arkansas serotype, respiratory disease was still occurring in chickens. The causative agent was identified as the IBV, Arkansas serotype, determined by virus neutralization (62). However, it was evident that the Arkansas viruses could in fact be distinguished genetically from one another. Four of the isolates Ark/213/96, Ark/15C/96, Ark/1529/95, Ark/1534/95 were genetically more closely related to each other than to the Arkansas-DPI reference strain (62).

More recently, the evolution of IBV giving rise to variants was shown with the California serotype of IBV. The Call99 variant was isolated from the kidneys of chickens with respiratory, as well as kidney disease. Upon sequencing the isolate, the S1 hypervariable region was 98% homologous to Cal99 thus they designated this new variant as IBV/CA99variant/07 (29). Previously, Cal99 has only been found to cause disease only in the respiratory tract thus indicating this variant has had a change in tissue tropism (26).

Genetic Resistance to Infectious Bronchitis Virus

Experimental infections have determined that the severity of the disease caused by IBV is dependent on the chicken breed (12). There are some chicken breeds that are resistant to IBV. While they are still susceptible to infection, resistant chickens recover much more quickly (63). In both resistant and susceptible breeds, immunohistochemical and ultra structural studies showed that the type of damage to the trachea epithelium following IBV infection was the same. However, the lesions were more severe and the infection lasted longer in the sensitive line (60). Using a T-cell suppressor, cyclosporin, in brown leghorn (BLH) chickens (a line of chickens that have been shown to be resistant to IBV) resulted in disease more like the sensitive lines of chickens. Normal BLH chickens that were infected with a pool of ten IBV strains, which produced 0% mortality. In contrast, immunesuppressed chickens showed 43% mortality (75). Other studies have directly linked the MHC haplotypes and the surrounding genes to genetic resistance against IBV (4).

The genes that encode MHC molecules in chickens are referred to as the B-complex. Located in this complex are genes that encode for three different MHC classes. The equivalent to human Class I is denoted BF, Class II is BL, and a novel Class III is BG, which has not been identified in mammals (49). The MHC B complex influences a variety of diseases and thus there will not be a single haplotype that responds optimally to all diseases (49). In addition, the lack of consistent association with certain haplotypes, corresponding to a specific response, leads one to believe that MHC linked genes rather

than the MHC I and II genes themselves may play a more pivotal role in resistance to certain diseases.

Diagnosis of IBV

Infectious Bronchitis Virus is commonly diagnosed based on clinical history, lesions in the birds, the presence of seroconversion of IBV antibodies, detection of IBV specific antigen, virus isolation, and detection of IBV RNA (14). The identification should include the serotype of the virus due to the antigenic differences between serotypes and the lack of cross reactivity. The use of RT-PCR to detect IBV RNA from tracheal swabs or cloacal swabs, is extremely sensitive. Due to its accuracy and speed, this method has largely replaced virus isolation in embryonated eggs. In addition, the hemagglutinin inhibition (HI) and Virus Neutralizations (VN) test are historically used to determine the serotype of the field virus (14). However, RT-PCR of the S1 gene followed by nucleotide sequencing has become the most widely used technique for differentiating IBV types. An added benefit to amplifying the viral RNA and sequencing the S1 gene is that universal primers can be used which amplify all IBV isolates enabling the identification of novel variants and serotypes (14).

Treatment of Infectious Bronchitis Virus

Currently, there is no treatment for IBV. Eliminating stressful conditions such as cold or overcrowding are two factors that can help reduce loss from the disease. Antibiotics can be given to reduce the chance of higher mortality due to secondary infections from bacterial pathogens. Lastly, electrolyte replacers can be given to compensate for the loss of sodium and potassium from nephritis (18).

References

- 1. Addie, D. D., S. A. McLachlan, M. Golder, I. Ramsey, and O. Jarrett. 2004. Evaluation of an in-practice test for feline coronavirus antibodies. J Feline Med Surg 6:63-7.
- 2. Addie, D. D., I. A. Schaap, L. Nicolson, and O. Jarrett. 2003. Persistence and transmission of natural type I feline coronavirus infection. J Gen Virol 84:2735-44.
- 3. An, S., C. J. Chen, X. Yu, J. L. Leibowitz, and S. Makino. 1999. Induction of apoptosis in murine coronavirus-infected cultured cells and demonstration of E protein as an apoptosis inducer. J Virol 73:7853-9.
- 4. Bacon, L. D., D. B. Hunter, H. M. Zhang, K. Brand, and R. Etches. 2004. Retrospective evidence that the MHC (B haplotype) of chickens influences genetic resistance to attenuated infectious bronchitis vaccine strains in chickens. Avian Pathol 33:605-9.
- 5. Baric, R. S., K. Fu, M. C. Schaad, and S. A. Stohlman. 1990. Establishing a genetic recombination map for murine coronavirus strain A59 complementation groups. Virology 177:646-56.
- 6. Barlough, J. E., R. H. Jacobson, C. E. Pepper, and F. W. Scott. 1984. Role of recent vaccination in production of false-positive coronavirus antibody titers in cats. J Clin Microbiol 19:442-5.
- 7. Benetka, V., A. Kubber-Heiss, J. Kolodziejek, N. Nowotny, M. Hofmann-Parisot, and K. Mostl. 2004. Prevalence of feline coronavirus types I and II in cats with histopathologically verified feline infectious peritonitis. Vet Microbiol 99:31-42.
- 8. Bo Chen, S. F., James P. Tam, Ding Xiang Liu. 2008. Formation of stable homodimer via the C-terminal Alpha-helical domain of coronavirus nonstructural protein 9 is critical for its function in viral replication. Virology.
- 9. Brown, M. A., J. L. Troyer, J. Pecon-Slattery, M. E. Roelke, and S. J. O'Brien. 2009. Genetics and pathogenesis of feline infectious peritonitis virus. Emerg Infect Dis 15:1445-52.
- 10. Casais, R., B. Dove, D. Cavanagh, and P. Britton. 2003. Recombinant avian infectious bronchitis virus expressing a heterologous spike gene demonstrates that the spike protein is a determinant of cell tropism. J Virol 77:9084-9.
- 11. Cavanagh, D. 2005. Coronaviridae: a review of coronaviruses and toroviruses. In A Schmidt, and Wolff, M., H (ed) Coronaviruses with special emphasisi on first insights concerning SARS Birkhauser, Basel, Switzerland.
- 12. Cavanagh, D. 2007. Coronavirus avian infectious bronchitis virus. Vet Res 38:281-97.
- 13. Cavanagh, D., R. Casais, M. Armesto, T. Hodgson, S. Izadkhasti, M. Davies, F. Lin, I. Tarpey, and P. Britton. 2007. Manipulation of the infectious bronchitis coronavirus genome for vaccine development and analysis of the accessory proteins. Vaccine 25:5558-62.

- 14. Cavanagh, D. a. G. J. J. 2008. Diseases of Poultry. 12th Edition:117-136.
- 15. Chen, H., A. Gill, B. K. Dove, S. R. Emmett, C. F. Kemp, M. A. Ritchie, M. Dee, and J. A. Hiscox. 2005. Mass spectroscopic characterization of the coronavirus infectious bronchitis virus nucleoprotein and elucidation of the role of phosphorylation in RNA binding by using surface plasmon resonance. J Virol 79:1164-79.
- 16. Cook, K. A., K. Otsuki, N. R. Martins, M. M. Ellis, and M. B. Huggins. 1992. The secretory antibody response of inbred lines of chicken to avian infectious bronchitis virus infection. Avian Pathol 21:681-92.
- 17. Corse, E., and C. E. Machamer. 2003. The cytoplasmic tails of infectious bronchitis virus E and M proteins mediate their interaction. Virology 312:25-34.
- 18. Cumming, R. B. 1969. The control of avian infectious bronchitis/nephrosis in Australia. Aust Vet J 45:200-3.
- 19. Davies, H. A., R. R. Dourmashkin, and M. R. Macnaughton. 1981. Ribonucleoprotein of avian infectious bronchitis virus. J Gen Virol 53:67-74.
- 20. de Groot-Mijnes, J. D., J. M. van Dun, R. G. van der Most, and R. J. de Groot. 2005. Natural history of a recurrent feline coronavirus infection and the role of cellular immunity in survival and disease. J Virol 79:1036-44.
- 21. de Haan, C. A., M. de Wit, L. Kuo, C. Montalto-Morrison, B. L. Haagmans, S. R. Weiss, P. S. Masters, and P. J. Rottier. 2003. The glycosylation status of the murine hepatitis coronavirus M protein affects the interferogenic capacity of the virus in vitro and its ability to replicate in the liver but not the brain. Virology 312:395-406.
- Decaro, N., D. Buonavoglia, C. Desario, F. Amorisco, M. L. Colaianni, A. Parisi, V. Terio, G. Elia, M. S. Lucente, A. Cavalli, V. Martella, and C. Buonavoglia.
 2010. Characterisation of canine parvovirus strains isolated from cats with feline panleukopenia. Res Vet Sci 89:275-8.
- 23. Delmas, B., J. Gelfi, R. L'Haridon, L. K. Vogel, H. Sjostrom, O. Noren, and H. Laude. 1992. Aminopeptidase N is a major receptor for the entero-pathogenic coronavirus TGEV. Nature 357:417-20.
- 24. Dong, B. Q., W. Liu, X. H. Fan, D. Vijaykrishna, X. C. Tang, F. Gao, L. F. Li, G. J. Li, J. X. Zhang, L. Q. Yang, L. L. Poon, S. Y. Zhang, J. S. Peiris, G. J. Smith, H. Chen, and Y. Guan. 2007. Detection of a novel and highly divergent coronavirus from asian leopard cats and Chinese ferret badgers in Southern China. J Virol 81:6920-6.
- Duarte, A., I. Veiga, and L. Tavares. 2009. Genetic diversity and phylogenetic analysis of Feline Coronavirus sequences from Portugal. Vet Microbiol 138:163-8.
- Dveksler, G. S., M. N. Pensiero, C. B. Cardellichio, R. K. Williams, G. S. Jiang, K. V. Holmes, and C. W. Dieffenbach. 1991. Cloning of the mouse hepatitis virus (MHV) receptor: expression in human and hamster cell lines confers susceptibility to MHV. J Virol 65:6881-91.
- 27. Eckerle, L. D., X. Lu, S. M. Sperry, L. Choi, and M. R. Denison. 2007. High fidelity of murine hepatitis virus replication is decreased in nsp14 exoribonuclease mutants. J Virol 81:12135-44.

- 28. Foley, J. E., A. Poland, J. Carlson, and N. C. Pedersen. 1997. Patterns of feline coronavirus infection and fecal shedding from cats in multiple-cat environments. J Am Vet Med Assoc 210:1307-12.
- 29. Franca, M., P. R. Woolcock, M. Yu, M. W. Jackwood, and H. L. Shivaprasad. 2011. Nephritis associated with infectious bronchitis virus Cal99 variant in game chickens. Avian Dis 55:422-8.
- 30. Gallardo, R. A., F. J. Hoerr, W. D. Berry, V. L. van Santen, and H. Toro. 2011. Infectious bronchitis virus in testicles and venereal transmission. Avian Dis 55:255-8.
- 31. Gallardo, R. A., V. L. van Santen, and H. Toro. 2010. Host intraspatial selection of infectious bronchitis virus populations. Avian Dis 54:807-13.
- 32. Gerber, J. D., J. D. Ingersoll, A. M. Gast, K. K. Christianson, N. L. Selzer, R. M. Landon, N. E. Pfeiffer, R. L. Sharpee, and W. H. Beckenhauer. 1990. Protection against feline infectious peritonitis by intranasal inoculation of a temperature-sensitive FIPV vaccine. Vaccine 8:536-42.
- 33. Gramberg, T., H. Hofmann, P. Moller, P. F. Lalor, A. Marzi, M. Geier, M. Krumbiegel, T. Winkler, F. Kirchhoff, D. H. Adams, S. Becker, J. Munch, and S. Pohlmann. 2005. LSECtin interacts with filovirus glycoproteins and the spike protein of SARS coronavirus. Virology 340:224-36.
- 34. Guan, Y., B. J. Zheng, Y. Q. He, X. L. Liu, Z. X. Zhuang, C. L. Cheung, S. W. Luo, P. H. Li, L. J. Zhang, Y. J. Guan, K. M. Butt, K. L. Wong, K. W. Chan, W. Lim, K. F. Shortridge, K. Y. Yuen, J. S. Peiris, and L. L. Poon. 2003. Isolation and characterization of viruses related to the SARS coronavirus from animals in southern China. Science 302:276-8.
- 35. Guy, J. S. 2008. Isolation and propagation of coronaviruses in embryonated eggs. Methods Mol Biol 454:109-17.
- 36. Haagmans, B. L., H. F. Egberink, and M. C. Horzinek. 1996. Apoptosis and T-cell depletion during feline infectious peritonitis. J Virol 70:8977-83.
- 37. Hartmann, K., C. Binder, J. Hirschberger, D. Cole, M. Reinacher, S. Schroo, J. Frost, H. Egberink, H. Lutz, and W. Hermanns. 2003. Comparison of different tests to diagnose feline infectious peritonitis. J Vet Intern Med 17:781-90.
- 38. Hawkes, R. A., J. H. Darbyshire, R. W. Peters, A. P. Mockett, and D. Cavanagh. 1983. Presence of viral antigens and antibody in the trachea of chickens infected with avian infectious bronchitis virus. Avian Pathol 12:331-40.
- 39. Herrewegh, A. A., M. Mahler, H. J. Hedrich, B. L. Haagmans, H. F. Egberink, M. C. Horzinek, P. J. Rottier, and R. J. de Groot. 1997. Persistence and evolution of feline coronavirus in a closed cat-breeding colony. Virology 234:349-63.
- 40. Herrewegh, A. A., I. Smeenk, M. C. Horzinek, P. J. Rottier, and R. J. de Groot. 1998. Feline coronavirus type II strains 79-1683 and 79-1146 originate from a double recombination between feline coronavirus type I and canine coronavirus. J Virol 72:4508-14.
- 41. Herrler, G., I. Durkop, H. Becht, and H. D. Klenk. 1988. The glycoprotein of influenza C virus is the haemagglutinin, esterase and fusion factor. J Gen Virol 69 (Pt 4):839-46.
- 42. Hodgson, T., R. Casais, B. Dove, P. Britton, and D. Cavanagh. 2004. Recombinant infectious bronchitis coronavirus Beaudette with the spike protein

- gene of the pathogenic M41 strain remains attenuated but induces protective immunity. J Virol 78:13804-11.
- 43. Holzworth, J. 1963. Infectious diseases of cats. Cornell Vet 53:131-43.
- 44. Hopkins, S. R., and H. W. Yoder, Jr. 1986. Reversion to virulence of chicken-passaged infectious bronchitis vaccine virus. Avian Dis 30:221-3.
- 45. Hurst, K. R., R. Ye, S. J. Goebel, P. Jayaraman, and P. S. Masters. 2010. An interaction between the nucleocapsid protein and a component of the replicase-transcriptase complex is crucial for the infectivity of coronavirus genomic RNA. J Virol 84:10276-88.
- 46. Jackwood, M. W., T. O. Boynton, D. A. Hilt, E. T. McKinley, J. C. Kissinger, A. H. Paterson, J. Robertson, C. Lemke, A. W. McCall, S. M. Williams, J. W. Jackwood, and L. A. Byrd. 2010. Emergence of a group 3 coronavirus through recombination. Virology 398:98-108.
- 47. Jackwood, M. W., D. A. Hilt, A. W. McCall, C. N. Polizzi, E. T. McKinley, and S. M. Williams. 2009. Infectious bronchitis virus field vaccination coverage and persistence of Arkansas-type viruses in commercial broilers. Avian Dis 53:175-83.
- 48. Jeffers, S. A., S. M. Tusell, L. Gillim-Ross, E. M. Hemmila, J. E. Achenbach, G. J. Babcock, W. D. Thomas, Jr., L. B. Thackray, M. D. Young, R. J. Mason, D. M. Ambrosino, D. E. Wentworth, J. C. Demartini, and K. V. Holmes. 2004. CD209L (L-SIGN) is a receptor for severe acute respiratory syndrome coronavirus. Proc Natl Acad Sci U S A 101:15748-53.
- 49. Kaufman, J., H. Volk, and H. J. Wallny. 1995. A "minimal essential Mhc" and an "unrecognized Mhc": two extremes in selection for polymorphism. Immunol Rev 143:63-88.
- 50. Kuo, L., and P. S. Masters. 2010. Evolved variants of the membrane protein can partially replace the envelope protein in murine coronavirus assembly. J Virol 84:12872-85.
- 51. Lorusso, A., N. Decaro, P. Schellen, P. J. Rottier, C. Buonavoglia, B. J. Haijema, and R. J. de Groot. 2008. Gain, preservation, and loss of a group 1a coronavirus accessory glycoprotein. J Virol 82:10312-7.
- 52. Maeda, J., A. Maeda, and S. Makino. 1999. Release of coronavirus E protein in membrane vesicles from virus-infected cells and E protein-expressing cells. Virology 263:265-72.
- 53. Maeda, J., J. F. Repass, A. Maeda, and S. Makino. 2001. Membrane Topology of Coronavirus E Protein. Virology 281:163-169.
- Marzi, A., T. Gramberg, G. Simmons, P. Moller, A. J. Rennekamp, M. Krumbiegel, M. Geier, J. Eisemann, N. Turza, B. Saunier, A. Steinkasserer, S. Becker, P. Bates, H. Hofmann, and S. Pohlmann. 2004. DC-SIGN and DC-SIGNR interact with the glycoprotein of Marburg virus and the S protein of severe acute respiratory syndrome coronavirus. J Virol 78:12090-5.
- 55. McKinley, E. T., D. A. Hilt, and M. W. Jackwood. 2008. Avian coronavirus infectious bronchitis attenuated live vaccines undergo selection of subpopulations and mutations following vaccination. Vaccine 26:1274-84.

- 56. Mihindukulasuriya, K. A., G. Wu, J. St Leger, R. W. Nordhausen, and D. Wang. 2008. Identification of a novel coronavirus from a beluga whale by using a panviral microarray. J Virol 82:5084-8.
- 57. Mochizuki, M., Y. Mitsutake, Y. Miyanohara, T. Higashihara, T. Shimizu, and T. Hohdatsu. 1997. Antigenic and plaque variations of serotype II feline infectious peritonitis coronaviruses. J Vet Med Sci 59:253-8.
- 58. Mockett, A. P., and J. K. Cook. 1986. The detection of specific IgM to infectious bronchitis virus in chicken serum using an ELISA. Avian Pathol 15:437-46.
- 59. Mondal, S. P., and S. A. Naqi. 2001. Maternal antibody to infectious bronchitis virus: its role in protection against infection and development of active immunity to vaccine. Vet Immunol Immunopathol 79:31-40.
- 60. Nakamura, K., J. K. Cook, K. Otsuki, M. B. Huggins, and J. A. Frazier. 1991. Comparative study of respiratory lesions in two chicken lines of different susceptibility infected with infectious bronchitis virus: histology, ultrastructure and immunohistochemistry. Avian Pathol 20:241-57.
- 61. Naqi, S., K. Gay, P. Patalla, S. Mondal, and R. Liu. 2003. Establishment of persistent avian infectious bronchitis virus infection in antibody-free and antibody-positive chickens. Avian Dis 47:594-601.
- 62. Nix, W. A., D. S. Troeber, B. F. Kingham, C. L. Keeler, Jr., and J. Gelb, Jr. 2000. Emergence of subtype strains of the Arkansas serotype of infectious bronchitis virus in Delmarva broiler chickens. Avian Dis 44:568-81.
- 63. Otsuki, K., M. B. Huggins, and J. K. Cook. 1990. Comparison of the susceptibility to avian infectious bronchitis virus infection of two inbred lines of white leghorn chickens. Avian Pathol 19:467-75.
- 64. Patel, J. R., and J. G. Heldens. 2009. Review of companion animal viral diseases and immunoprophylaxis. Vaccine 27:491-504.
- 65. Pedersen, N. 1995. An Overview of Feline Enteric Coroanvirus and Infectious Peritonitis Virus Infections. Department of Medicine and Epidemiology School of Veterinary Medicine University of California.
- 66. Pedersen, N. C. 2009. A review of feline infectious peritonitis virus infection: 1963-2008. J Feline Med Surg 11:225-58.
- 67. Pedersen, N. C., J. F. Boyle, K. Floyd, A. Fudge, and J. Barker. 1981. An enteric coronavirus infection of cats and its relationship to feline infectious peritonitis. Am J Vet Res 42:368-77.
- 68. Pedersen, N. C., R. Sato, J. E. Foley, and A. M. Poland. 2004. Common virus infections in cats, before and after being placed in shelters, with emphasis on feline enteric coronavirus. J Feline Med Surg 6:83-8.
- 69. Pedersen, N. C., J. Ward, and W. L. Mengeling. 1978. Antigenic relationship of the feline infections peritonitis virus to coronaviruses of other species. Arch Virol 58:45-53.
- 70. Pei, J., W. E. Briles, and E. W. Collisson. 2003. Memory T cells protect chicks from acute infectious bronchitis virus infection. Virology 306:376-84.
- 71. Pensaert, M. B., and P. de Bouck. 1978. A new coronavirus-like particle associated with diarrhea in swine. Arch Virol 58:243-7.

- 72. Popova, R., and X. Zhang. 2002. The spike but not the hemagglutinin/esterase protein of bovine coronavirus is necessary and sufficient for viral infection. Virology 294:222-36.
- 73. Potkay, S., J. D. Bacher, and T. W. Pitts. 1974. Feline infectious peritonitis in a closed breeding colony. Lab Anim Sci 24:279-89.
- 74. Raj, G. D., and R. C. Jones. 1997. Cross-reactive cellular immune responses in chickens vaccinated with live infectious bronchitis virus vaccine. Avian Pathol 26:641-9.
- 75. Raj, G. D., and R. C. Jones. 1997. Effect of T-cell suppression by cyclosporin on primary and persistent infections of infectious bronchitis virus in chickens. Avian Pathol 26:257-76.
- 76. Risco, C., I. M. Anton, L. Enjuanes, and J. L. Carrascosa. 1996. The transmissible gastroenteritis coronavirus contains a spherical core shell consisting of M and N proteins. J Virol 70:4773-7.
- 77. Rossen, J. W., J. Kouame, A. J. Goedheer, H. Vennema, and P. J. Rottier. 2001. Feline and canine coronaviruses are released from the basolateral side of polarized epithelial LLC-PK1 cells expressing the recombinant feline aminopeptidase-N cDNA. Arch Virol 146:791-9.
- 78. Schultze, B., and G. Herrler. 1992. Bovine coronavirus uses N-acetyl-9-O-acetylneuraminic acid as a receptor determinant to initiate the infection of cultured cells. J Gen Virol 73 (Pt 4):901-6.
- 79. Seo, S. H., and E. W. Collisson. 1997. Specific cytotoxic T lymphocytes are involved in in vivo clearance of infectious bronchitis virus. J Virol 71:5173-7.
- 80. Sharif, S., S. S. Arshad, M. Hair-Bejo, A. R. Omar, N. A. Zeenathul, and A. Alazawy. 2010. Diagnostic methods for feline coronavirus: a review. Vet Med Int 2010.
- 81. Snijder, E. J., P. J. Bredenbeek, J. C. Dobbe, V. Thiel, J. Ziebuhr, L. L. Poon, Y. Guan, M. Rozanov, W. J. Spaan, and A. E. Gorbalenya. 2003. Unique and conserved features of genome and proteome of SARS-coronavirus, an early split-off from the coronavirus group 2 lineage. J Mol Biol 331:991-1004.
- 82. Sparkes, A. H., T. J. Gruffydd-Jones, and D. A. Harbour. 1991. Feline infectious peritonitis: a review of clinicopathological changes in 65 cases, and a critical assessment of their diagnostic value. Vet Rec 129:209-12.
- 83. Stoddart, C. A., and F. W. Scott. 1989. Intrinsic resistance of feline peritoneal macrophages to coronavirus infection correlates with in vivo virulence. J Virol 63:436-40.
- 84. Stoddart, M. E., R. M. Gaskell, D. A. Harbour, and C. J. Gaskell. 1988. Virus shedding and immune responses in cats inoculated with cell culture-adapted feline infectious peritonitis virus. Vet Microbiol 16:145-58.
- 85. Tang, X., G. Li, N. Vasilakis, Y. Zhang, Z. Shi, Y. Zhong, L. F. Wang, and S. Zhang. 2009. Differential stepwise evolution of SARS coronavirus functional proteins in different host species. BMC Evol Biol 9:52.
- 86. Thor, S., Phillips, JE., Hilt, DA., Kissinger, J., Paterson, A., Jackwood, MW. 2010. Poster Presentation, "Molecular Characterization of a nephropathogenetic Infectious Bronchitis Virus Genome: Clues to tissue tropism. Southern Conference of Avian Diseases.

- 87. USDA. 1999. Title 9, Code of Federal Regulations, Standard Requirements for IBV Vaccines. Animal and Plant Health Inspection Service, U.S. National Archives and Records Administration College Park, MD.
- 88. Van Hamme, E., L. Desmarets, H. L. Dewerchin, and H. J. Nauwynck. 2011. Intriguing interplay between feline infectious peritonitis virus and its receptors during entry in primary feline monocytes. Virus Res 160:32-9.
- 89. Vijgen, L., E. Keyaerts, E. Moes, I. Thoelen, E. Wollants, P. Lemey, A. M. Vandamme, and M. Van Ranst. 2005. Complete genomic sequence of human coronavirus OC43: molecular clock analysis suggests a relatively recent zoonotic coronavirus transmission event. J Virol 79:1595-604.
- 90. Weiss, R. C., and F. W. Scott. 1981. Antibody-mediated enhancement of disease in feline infectious peritonitis: comparisons with dengue hemorrhagic fever. Comp Immunol Microbiol Infect Dis 4:175-89.
- 91. Winter, C., C. Schwegmann-Wessels, D. Cavanagh, U. Neumann, and G. Herrler. 2006. Sialic acid is a receptor determinant for infection of cells by avian Infectious bronchitis virus. J Gen Virol 87:1209-16.
- 92. Wolfe, L. G., and R. A. Griesemer. 1966. Feline infectious peritonitis. Pathol Vet 3:255-70.
- 93. Woo, P. C., S. K. Lau, Y. Huang, and K. Y. Yuen. 2009. Coronavirus diversity, phylogeny and interspecies jumping. Exp Biol Med (Maywood) 234:1117-27.
- 94. Woo, P. C., S. K. Lau, C. S. Lam, K. K. Lai, Y. Huang, P. Lee, G. S. Luk, K. C. Dyrting, K. H. Chan, and K. Y. Yuen. 2009. Comparative analysis of complete genome sequences of three avian coronaviruses reveals a novel group 3c coronavirus. J Virol 83:908-17.
- 95. Ye, Y., K. Hauns, J. O. Langland, B. L. Jacobs, and B. G. Hogue. 2007. Mouse hepatitis coronavirus A59 nucleocapsid protein is a type I interferon antagonist. J Virol 81:2554-63.
- 96. Ziebuhr, J., V. Thiel, and A. E. Gorbalenya. 2001. The autocatalytic release of a putative RNA virus transcription factor from its polyprotein precursor involves two paralogous papain-like proteases that cleave the same peptide bond. J Biol Chem 276:33220-32.

CHAPTER 3

COMPARATIVE ANALYSIS OF NONSTRUCTURAL PROTEIN 14 IN THE REPLICATION TRANSCRIPTION COMPLEX OF INFECTIOUS BRONCHITIS ${\sf VIRUS}^1$

 1 Phillips, J.E., Hilt, D.A., and Jackwood, M.W. To be submitted to $\it Virus \ Genes$

ABSTRACT

Coronaviruses (CoVs) have an extensive replication transcription complex (RTC) that mediates transcription and replication at double membrane vesicles in the cytoplasm. Although the actual mechanism and enzymes involved have yet to be completely elucidated, nonstructural protein 14 (nsp 14) has been shown for the alpha and beta coronaviruses to have exoribonuclease (EXON) as well as a methyltransferase (MTase) activity. The presence of the EXON domain in this protein indicates that CoVs may have some degree of proof reading capability. We sequenced the nsp 14 from several gammacoronavirus infectious bronchitis virus (IBV) strains and compared them to the alpha and beta CoV nsp 14 sequences to determine if the predicted active site of the EXON was conserved in the gammacoronaviruses. We identified multiple conserved residues particularly the DEDD motif that indicate IBV likely has some degree of proofreading activity similar to the alpha and beta CoVs.

INTRODUCTION

The RNA viruses strike a balance between mutations necessary for adapting to the host while also maintaining conserved regions in all the genes necessary for replication. This balance is even more challenging for CoVs, which have the largest genome of all RNA viruses and have a greater possibility of deleterious mutations. Infectious Bronchitis Virus (IBV), a gammacoronavirus, causes a highly contagious upper-respiratory disease in chickens. The viral genome is approximately 27kb. The polyproteins 1a and 1ab make up the first two-thirds of the genome, and in the gammacoronaviruses, get posttranslationally cleaved into 15 nonstructural proteins (nsps) that form the replication transcription complex (RTC). The alpha and beta coronaviruses have 16 nsps (gammacoronaviruses lack nsp 1). The exact mechanism of how the RTC forms is unclear but, during replication, it is thought to shield the viral RNA from the host cell's innate immune response. Based on homology and some mutational studies, several CoV nsps have been functionally characterized. The autolytic process of 1a/ab is mediated by a papain like protease(s) (PLP(s)) in nsp 3, and a main protease (Mpro) located in nsp 5 (6). The nsp 2, 4, and 6 are thought to tether the RTC together due to their hydrophobic domains. Nonstructural proteins 7 to 10 are thought to play a role in RNA binding activity, and nsp 9 is thought to play a role in viral replication. The RNA dependent RNA polymerase is located in nsp 12. Nonstructural protein 13 is a helicase and nsp 14 is an exoribonuclease (EXON)/methyltransferase (MTase). Nonstructural protein 15 is an endoribonuclease and nsp 16 is a MTase.

Located downstream of the predicted RNA-dependent RNA polymerase and upstream from a predicted endoribonuclease, the nsp 14 protein is predicted to be cleaved by nsp 5 (Mpro) and is thought to serve as an intermediate precursor for replication of the virus (5). The nsp 14 has several domains, which include three motifs that make up the EXON domain, a zinc finger, and MTase domain (7, 8) (Fig. 3.1.). It is thought that this protein degrades RNA by removing terminal nucleotides from either the 5' end or the 3' end, enabling the polymerase to have some type of proof reading capability. This proof

reading capability is thought to be similar to the proof reading found in eukaryotic RNA pol II and bacterial RNA (3). As evidence, deletion of nsp 14 resulted in a >94% reduction of RNA synthesis in cells that were infected with severe acute respiratory syndrome-CoV (SARS-CoV) replicons (1). In addition, alanine substitutions were made in the EXON domain of human coronavirus 229E (HCoV-229E), which severely reduced the amount of viral RNA synthesis (7). Alternatively, when alanine substitutions were made in mouse hepatitis virus (MHV) and SARS-CoV viable mutants were recovered (3, 7).

The majority of the work examining proof reading capability in coronaviruses has been done in alpha- and beta- CoVs. In this study, we examined the sequences of nsp 14 from six different gammacoronaviruses and compared those to nsp 14 sequences from alpha- and beta- CoVs to determine if EXON sequences are conserved in the gammacoronavirus group.

RESULTS

All viruses analyzed in this study are listed in Table 3.1 along with their NCBI accession number (http://www.ncbi.nlm.nih.gov/). Motifs I, II and III, located in the EXON, were found to be conserved across all groups of CoV (Fig. 3.1.). Although the sequences had less than or equal to 50% identity between FCoV, SARS-CoV, MHV, and IBV, the DEDD core sequence was conserved (Fig. 3.2). In addition, one amino acid difference was observed in the zinc finger at position 208; SARS-CoV had an L insertion and MHV had a V insertion. Residues 330 D and 332 G were conserved among all viruses examined in this study, these residues are located in the MTase domain and are putative SAM-binding sites. Residues located at the C-term, F-W-N-C-N-V-D (385-392) and L-Y-V-N-(K/N)-H-A-F (411-419) are highly conserved across all groups but have no known homologs.

The sequences of the gammacoronaviruses were highly conserved. The Massachusetts 41 pathogenic strain differed from the other gammacoronaviruses by only one amino acid at V243I and the Mass 41 vaccine strain differed from the other gammacoronaviruses at two positions; V205L and V243I.

DISCUSSION

The presence of a 3' to 5' EXON domain is conserved in coronaviruses, toroviruses, and the roniviridae, but not in the arteriviridae (8). In MHV strain A59, a single amino acid substitution in nsp 14 attenuated the virus in mice (4). Based on its sequence homology with other proteins, such as the host cellular proteins of the DEDD superfamily of exonucleases, it is predicted to play an important role in replication with regard to mutation rates, and affect proofreading and repair (8). All DEDD family exonucleases have an active site that contains four acidic amino acids that interact with two divalent metal ions and several water molecules (9). The zinc finger, which is a proposed nucleic acid binding domain, is predicted to be located between motifs I and II.

Another important domain of the nsp 14 is the MTase, which plays a role in the capping of the RNAs and is located at the carboxy terminus of the nsp 14 protein. The active sites of the EXON and the MTase are independent of one another, but the EXON domain is necessary for the functionality of the MTase domain (2). Site directed mutagenesis studies that altered, or deleted, these motifs in a betacoronavirus Group IIb virus showed that the defects caused reduced genome replication and increase mutations in the synthesis of subgenomic RNAs (3).

We found that these domains are conserved in IBV, which indicates that like the alpha and beta CoVs, gammacoronaviruses may posses some proofreading activity.

The majority of RNA viruses have high mutation rates, which results in many nucleotide changes both beneficial and deleterious. However, the predicted proof reading activity of this viral protein would explain why CoVs have high mutation rates yet maintain their large genomes and exist below the threshold of mutational death. The ability to control replication fidelity is unique among CoVs and understanding the mechanism behind the EXON domain will be key in the control of this important group of RNA viruses.

References

- Almazan, F., M. L. Dediego, C. Galan, D. Escors, E. Alvarez, J. Ortego, I. Sola, S. Zuniga, S. Alonso, J. L. Moreno, A. Nogales, C. Capiscol, and L. Enjuanes. 2006. Construction of a severe acute respiratory syndrome coronavirus infectious cDNA clone and a replicon to study coronavirus RNA synthesis. J Virol 80:10900-6.
- 2. Chen, Y., H. Cai, J. Pan, N. Xiang, P. Tien, T. Ahola, and D. Guo. 2009. Functional screen reveals SARS coronavirus nonstructural protein nsp14 as a novel cap N7 methyltransferase. Proc Natl Acad Sci U S A 106:3484-9.
- 3. Denison, M. R., R. L. Graham, E. F. Donaldson, L. D. Eckerle, and R. S. Baric. 2011. Coronaviruses: an RNA proofreading machine regulates replication fidelity and diversity. RNA Biol 8:270-9.
- 4. Eckerle, L. D., X. Lu, S. M. Sperry, L. Choi, and M. R. Denison. 2007. High fidelity of murine hepatitis virus replication is decreased in nsp14 exoribonuclease mutants. J Virol 81:12135-44.
- 5. Graham, R. L., J. S. Sparks, L. D. Eckerle, A. C. Sims, and M. R. Denison. 2008. SARS coronavirus replicase proteins in pathogenesis. Virus Res 133:88-100.
- 6. Imbert, I., E. J. Snijder, M. Dimitrova, J. C. Guillemot, P. Lecine, and B. Canard. 2008. The SARS-Coronavirus PLnc domain of nsp3 as a replication/transcription scaffolding protein. Virus Res 133:136-48.
- 7. Minskaia, E., T. Hertzig, A. E. Gorbalenya, V. Campanacci, C. Cambillau, B. Canard, and J. Ziebuhr. 2006. Discovery of an RNA virus 3'->5' exoribonuclease that is critically involved in coronavirus RNA synthesis. Proc Natl Acad Sci U S A 103:5108-13.
- 8. Snijder, E. J., P. J. Bredenbeek, J. C. Dobbe, V. Thiel, J. Ziebuhr, L. L. Poon, Y. Guan, M. Rozanov, W. J. Spaan, and A. E. Gorbalenya. 2003. Unique and conserved features of genome and proteome of SARS-coronavirus, an early split-off from the coronavirus group 2 lineage. J Mol Biol 331:991-1004.
- 9. Zuo, Y., H. Zheng, Y. Wang, M. Chruszcz, M. Cymborowski, T. Skarina, A. Savchenko, A. Malhotra, and W. Minor. 2007. Crystal structure of RNase T, an exoribonuclease involved in tRNA maturation and end turnover. Structure 15:417-28.

Table 3.1. Viruses examined in this study with corresponding accession numbers.

Viruses	Accession Number
Ark-attenuated (Mildvac-Ark)	GQ504721
Ark/Ark-DPI/81	GQ504720
GA98- attenuated (Mildvac-Ga-98)	GQ504723
GA98/CWL0470/98	GQ504722
Mass41-attenuated (Mildvac-H)	GQ504725
Mass/Mass41/41 pass 8	GQ504724
putative ORF1ab polyprotein [SARS coronavirus FRA	AAP50483.1
nsp14; exoribonuclease [Murine hepatitis virus strain JHM]	YP_209241.1
FCoV/FIPV/FCoVWSu79-1146p8	*

^{*}No accession number assigned, sequenced in Jackwood lab

Nonstructural Protein 14

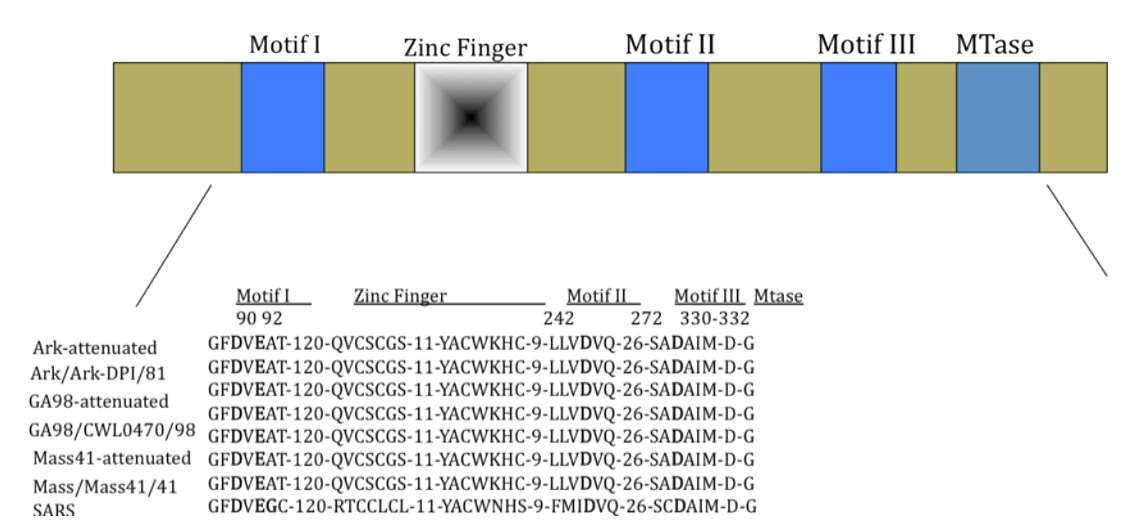


Figure 3.1 Schematic diagram of nsp 14 showing the organization of domains as found in the sArk/Ark-DPI/81 (GQ504720); Ark-attenuated (GQ504721); GA98/CWL0470/98 (GQ504722); GA98-attenuated (GQ50 4723); Mass/Mass41/41 (GQ504724); and Mass41-attenuated (GQ504725), and SARS (AAP50483.1). The EXON motifs are highlighted in blue and a putative zinc finger is shown in black. The highly conserved DEDD residues in the the EXON active site are shown in bold and the corresponding amino acid numbers are listed below. Motif's I, II and III were highly conserved across the gammacoronaviruses.

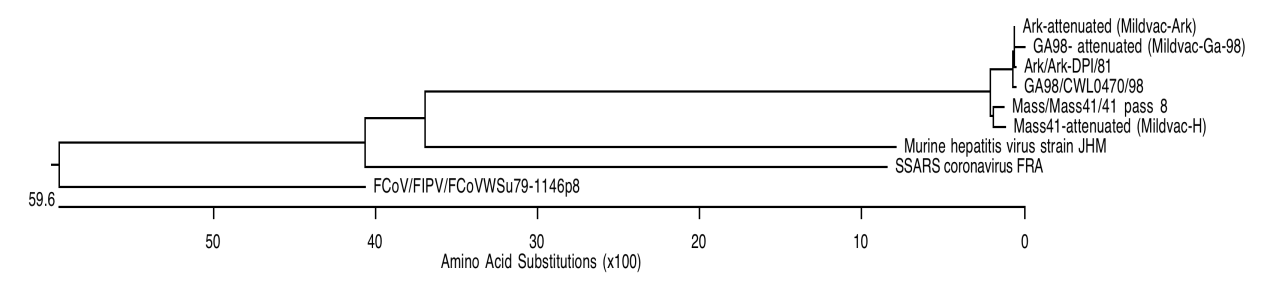


Figure 3.2 Phylogenetic tree of nonstructural protein 14 created using DNASTAR. These data show that nsp 14 is not genetically similar among the different CoV groups however; based on amino acid comparisons the EXON active sites are conserved.

CHAPTER 4

MOLECULAR CHARACTERIZATION OF FELINE INFECTIOUS PERITONITIS VIRUS: COMPARATIVE SEQUENCE ANALYSIS OF FULL-LENGTH GENOMES OF FIPV AT DIFFERENT TISSUE PASSAGES 2

² Phillips, J.E., Hilt, D.A., and Jackwood, M.W. To be submitted to *Veterinary Microbiology*

ABSTRACT

Feline coronavirus occurs in two biotypes, feline enteric coronavirus virus (FECV), which causes a mild enteric disease in cats and feline infectious peritonitis virus (FIPV), which causes a typically fatal systemic disease. The relationship between the two biotypes is not clear but one theory maintains that mutations in FECV lead to the emergence of FIPV. To better understand the capacity of FCoV to change genetically, we sequenced the full-length genome of the virus at tissue culture passage levels 1, 9, and 51 and we conducted growth curve analysis for each passage as a measure of viral adaptation. Although the viruses were 99.9% similar across the entire genome, some changes were observed. Twenty-one amino acid differences were observed in the polyprotein 1a/ab. Only 1 residue change was observed in the spike glycoprotein, which reverted back on subsequent passages, four changes were observed in the 3c protein, and one change was observed in each the 3a, small membrane, nucleocapsid and 7a protein. Growth curve analysis revealed that little or no change in the growth kinetics occurred for any of the passages. Taken together, these data show that little or no change occurred in FCoV following passage in cell culture indicating that FECV is relatively stable in vitro.

Keywords: Feline Infectious Peritonitis Virus, Feline Enteric Coronavirus, Pathogenicity, Genomic Sequencing, and FIPV

INTRODUCTION

Coronaviruses are in the order Nidovirales, family Coronaviridae and are divided into alpha, beta, and gamma subgroups based on genetic and antigenic differences. Feline coronavirus (FCoV) is classified in the alphacoronavirus group and is found in domestic cats worldwide.

Feline Coronaviruses can be divided into two groups: type I and type II. Type I viruses are considered to be "wholly" feline, whereas the type II viruses have been identified as recombinants between Canine Coronavirus (CCoV) and type I FCoV (13). Within the type II FCoV, separate recombination events have occurred between the CCoV and the type I FCoV. Type I causes the majority of natural infections but most studies have focused on type II viruses, because they can be propagated in cell culture (20). The current geographical distribution of FCoV indicates that Europe, Japan and the US have a high incidence of Type I FCoV (7), whereas type II viruses make up more than 30% of isolates in Japan (18). Approximately 40% of cats have been infected with FCoV in the UK however, this number may more than double in multi-cat households (8).

There are two biotypes of FCoV; FECV and FIPV. The majority of FCoV infections are transient; however some become persistent (1). The majority of infections result in a mild gastrointestinal disease with the causative agent identified as FECV. Some infections can result in a fatal disease caused by FIPV. The feline infectious peritonitis virus affects domestic cats, and has also been identified in other animals such as the African lion (Panthera leo), the mountain lion (Puma concolor), leopard (Panthera pardus), and the cheetah (Acinonyx jubatus) (9). The wild type FIPV strain 79-1146 is extremely virulent, resulting in 70-90% mortality when inoculated intranasally (12).

In 1996, Poland *et al.* suggested that cats acquire FIPV by mutations that occur in an endogenous FECV (22). This is known as the "*in vivo* mutation transition hypothesis" which is defined by the FECV disseminating from the gut, and becoming systemic via *de novo* virus mutations (3, 17). The conversion from FECV to FIPV is thought to occur more frequently in a primary infection and in cats >1 year of age (18). The exact change that enables the virus to replicate more efficiently in macrophages is not clear. Truncation

in the 3C gene has been proposed, which encodes a small protein of unknown function, causes the change in cell tropism (19). However, other studies suggest that changes in spike as well as the 7b protein play a role in the pathotype (14, 21). Specific mutations can differ between FIPV isolates from affected kittens in the same litter (19). This data supports that internal mutations to the virus result in FIPV as opposed to horizontal transmission from cat to cat.

A second hypothesis postulates that there are two circulating, similar viruses that cause different diseases. One study looked at four regions within the genome: the spike-3a-3c (1,017 bp), membrane (575 bp), polymerase (384 bp) and 7b (735bp) in order to demonstrate distinctive circulating virulent and avirulent strains in natural populations (4). Based on their phylogenetic analysis, they concluded there is clear genetic differentiation between viruses that cause FIP and FECV cats in multiple gene segments. Thus cats are re-infected with different strains of the virus from external sources (4). It may be possible that both hypotheses contribute to the development of FIP.

Regardless of which hypothesis is correct, the capacity of the virus to change likely plays a key role in the pathogenesis of the virus. As a first step in identifying the capacity of FIPV to genetically change, we examined the sequence of the full-length genome identifying changes that occurred with passage in a laboratory host. In addition, the growth kinetics for the virus at different tissue passage levels was examined as a measure of viral adaptation to cell culture.

MATERIAL AND METHODS

Cells and Viruses

The three viruses sequenced in this study FCoV/FIPV/FCoVWSU 79-1146 passage 1, FCoV/FIPV/FCoVWSU79-1146 TC passage 8, and FCoV/FIPV/FCoVWSU79-1146 TC passage 50. These viruses were obtained from ATCC (Manassas, VA 2010). A-72 canine epithelial kidney cells (ATCC CRL-1542) were obtained from Dr. J. Saliki at the University of Georgia (Athens, GA). Cells were maintained in Dulbecco's modified eagles medium (DMEM) supplemented with 10%

fetal bovine serum (FBS). Cells were then cultured in a 37° degree incubator in 5% CO₂. Working stocks of virus were produced in A72 cells and quantified by plaque assay.

Viral RNA extraction and RT-PCR

Viral RNA was purified using the High Pure RNA Isolation Kit according to the manufacturer's recommendation (Roche Diagnostic Corporation, Foster City, CA) and re-suspended in DEPC treated water. Specific primers were synthesized (Integrated DNA Technologies, Coralville, IA) for RT-PCR amplification and sequencing based on the published FCoV sequences on Genebank. The RT-PCR conditions were 42°C for 60 minutes, 95°C for five minutes, then ten cycles of 94°C for 30 seconds, 50°C for 30 seconds, 68°C for 90 seconds, followed by 25 cycles of 94°C for 30 seconds, 50°C for 30 seconds, 68°C for 90sec, plus 5sec/cycle added. The final elongation step was 68°C for 7 minutes then the reaction was cooled to 4°C. The PCR products were sequenced in both directions using the ABI Prism BigDye Terminator v3.0 (Applied Biosystems, Foster City Ca) and the specific primers that were used for amplification at a concentration of 15ng. The amount of cDNA added to the reaction ranged from 20-30ng and the sequencing reactions were analyzed on an ABI 3730 (Applied Biosystems).

Sequencing alignment and nonstructural protein comparison

Chromatogram files and trace data were read and assembled using SeqMan Pro, and genome annotation was conducted with SeqBuilder (DNASTAR, Inc., v.8.0.2, Madison, WI). The sequences were assembled using SeqMan Pro, and genome annotation was conducted with SeqBuilder (DNASTAR, Inc., v.8.0.2, Madison, WI). Full-length genomes were uploaded to NCBI ORF finder (http://www.ncbi.nlm.nih.gov/gorf/gorf.html) to identify open reading frames. Nucleotide and deduced amino acid alignments were assembled using Clustal W in the MegAlign program (DNASTAR, Inc.).

Virus titration and viral growth curves

Viruses were grown in A72 cells (passed one time before use), and infected at a multiplicity of infection of 0.1. The viral inoclum was removed after a 1 hour incubation at 37°C and maintenance media was added. Growth curves of the isolates examined in this study were performed in A72 kidney canine cells. The culture supernatant was harvested every twelve hours after inoculation. To investigate the viral titer in the cells at the time of harvest, the cells were frozen and thawed three times then filtered. The viral titers were determined by plaque assay. Plaque assays were performed by inoculating monolayers of A72 cells in six well plates with 200ul of ten-fold serial dilutions of the virus. The virus was adsorbed for 1 hour at 37°C then removed and the cells were overlaid with 2ml of maintenance media containing 0.08% agarose (Lonza Rockland, ME). Monolayers were checked daily for plaques. All dilutions for every time point were performed in triplicate.

RESULTS

Genomic sequence of FCoV WSU 79-1146

The genomes for all three viruses sequenced in this study were found to be 99.9% similar at the nucleotide level. The gene order was found to be consistent with previous findings 5'-UTR- 1a/1ab-S-3a-3b-3c-E-M-N-7a-7b-3'-UTR. The viruses at all passage levels had a genome size of 29,357, and the nucleotide composition was found to be A=29.21%, G=21.02%, T=32.64, and C=17.12% for the WSU 79-1146 strain.

ORFs and expression products

A total of 21 site differences were detected in the polyproteins 1a and 1ab between the viruses sequenced in this study. The exact amino acid changes are presented in Table 4.1. Nonstructural protein 1, 11, 15, and 16 had no amino acid differences. Nonstructural protein 2, which is predicted to serve as a tethering protein due to its,

predicted trans-membrane domains, had 3 amino acid differences. Residue 177 changed from an aspartic acid to glycine in FCoV passage 8, and this change was present at passage 50 and 100. A second amino acid change from tryptophane to cysteine occurred at position 388 however, this change occurred between passage 8 and passage 50 and then was maintained in passage 100. The third amino acid change in nsp 2 was a lysine to threonine at position 807 in passage100. Nonstructural protein 13 had one amino acid change from aspartic acid to valine at position 5050 that occurred after passage 1, and was maintained in subsequent passages. Other amino acid differences that occurred in the polyproteins 1a/ab, which were reversions, are listed in Table 4.2.

Structural and Accessory Proteins

The Spike protein is 1452 amino acids in length and had only one change at residue 599 from threonine to an alanine at passage 8, which reverted back by passage 50. When compared to the FIPV WSU79-1146p100, two additional amino acid changes were observed; alanine to valine at position 743, and argenine to glutamic acid at position 1325.

The accessory protein 3a had one amino acid change from phenylalanine to serine at position 61 but this change was not maintained and by passage 50 reverted back to phenylalanine. Accessory protein 3b had no amino acid differences, while protein 3c had four changes, at position 25 valine to glycine, which reverted back by pass50, at position 35 phenylalanine to leucine between passage 8-passage 50, and at position 42 tyrosine to isoleucine at passage 8, which reverted back by passage 50. The fourth change in this accessory protein occurred at position 52 where asparagine changed to a histidine but this change also reverted back by passage 50. Comparing passage 100 to the earlier passages, a 15 amino acid rearrangement occurred where the sequence between position 33 and 57 (LTLHFVDPMLVRIAI) in the earlier passages was translocated to position 106 to 120 (Fig 4.1).

The small envelope protein has one amino acid change from isoleucine to threonine at position 71 that was maintained in consecutive passages. The membrane, nucelocapsid, and the 7a protein had no amino acid changes in the early passages but in

passage 100 the nucleocapsid protein had one change from lucine to arginine at position 18, and protein 7a had one amino acid change, from leucine to methionine at position 39. The 7b protein, which starts at nucleotide position 28,462-29,082 and is 206 amino acids in length, was found to be truncated at passage 50 resulting in a 48 amino acid protein, also observed in passage 100 (Table 4.2).

N-linked Glycosylation of the Spike Glycoprotein

The spike glycoproteins for all three viruses sequenced in this study were analyzed for predicted glycosylation sites using the NetNGlyc 1.0 Server (http://www.cbs.dtu.dk/services/NetNGlyc/), and the prediction algorithm indicated that there were 13 potential N-linked glycosylation sites at positions 29, 67, 95, 174, 234, 348, 408, 519, 535, 783, 822, 843, and 1361 (Fig. 4.2).

Comparison with other Group I CoV

Phylogenetic analysis (Fig. 4.3) on the virus strains listed in Table 4.3 showed that the three strains sequenced in this study group closely together (approximately 99.8 or 99.9% similarity) along with the FCoV/FIPV79-1146/USA passage 100 (accession number DQ010921). The FCoV/DF-2/USA virus (accession number DQ286389) also fell into the same clade (approximately 99.2% similarity) and all are type II viruses. The FCoV/DF-2/USA virus is a live attenuated vaccine. The other FIPV viruses included in the analysis are, FCoV/FECV/Black/1970 strain (accession number EU186072), which had approximately 88% similarity, FCoV/FIPV/C1JE (accession number DQ848678.1), which had 83.6% similarity, and FCoV/INTU156p/2007 (accession number GQ152141), which had 92.2% similarity, when aligned to the viruses sequenced in this study. The Canine CoV/NTU336/F/2008 and the TGEV/Purdue/Pur46-Med and TGEV/Purdue/P126 also grouped with the Type II FCoV. Because these viruses have close genetic similarity in the 1ab region the International Committee of Taxonomy of Viruses declared that these viruses should be considered host range variants of the same species, and not separate viruses (6).

Polyprotein 1a, which comprises the first 10,000 nucleotides of the WSU 79-1146 genome was found to be feline like having 82% sequence similarity or greater to other FCoV (Fig. 4.4 box I.). Interestingly, Simplot analysis also suggested that group II FCoVs are more closely related to TGEV, CCoV, and PRCV than to Type I FCoV (Fig. 4.4 Box II). The feline CoV type II have high sequence similarity in the S protein to CCoV, TGEV, and PRCV (approximately 90% or greater) (Fig. 4.4 Box III). The 3' end of the genome, more specifically N and 7ab genes appear to be FCoV group specific and diverge from the CCoV, TGeV, and PRCV (Fig. 4.4 Box IV).

The Feline WSU 79-1146 pass 1 virus was compared to the Feline RM strain, an enteric virus (FJ938051.1) from California. The RM strain does not induce FIP however; two virus's FIPC-UCD9 and UCD10 are FIPV mutants that have almost complete genetic similarity, based on the sequence analysis of ORF 7, to each other and to the FCoV RM. The two closely related FIPV strains have not yet been sequenced but the full-length genome of the RM strain has. It is for this reason a comparison was made with the FIPV 79-1146 virus that was sequenced in our lab. The RM and FCoV WSU 79-1146 had approximately 86.2% similarity at the nucleotide level. The polyproteins 1a and 1ab were found to have 94.8% sequence similarity at the amino acid level. The Spike proteins had 47.3% sequence similarity at the amino acid level. Protein 3a contained 22 amino acid differences. Protein 3b was 100% identical at the amino acid level and protein 3c differed by 24 amino acids. However, the 3C in the FIPV strain was truncated when compared to the RM strain, which had 73 amino acids more at the N-term comparatively. The envelope protein comparison yielded 3 amino acid differences, the membrane yielded 10 amino acid differences and the nucelocapsid protein had 28 amino acid differences. The 7a protein was truncated in the RM strain by 7 amino acids and 12 differences were found throughout the protein. Lastly, 18 differences were found in protein 7b.

Growth Curve

The growth curve analysis of FCoV/FIPV/FCoVWSU97-1146 passage 2, passage 9 and passage 51 were performed in canine A-72 cells (Figure 4.5.). At passage- 2, virus reached a peak titer of 1 X 10¹¹ PFUs at 84 hours post inoculation, whereas the peak titer

of passage- 9 was 1 X 10⁷ PFUs at 48 hours post-inoculation and passage- 51 had a peak titer of 1 X 10⁸ PFUs at 84 hours post-inoculation. Statistical analysis was performed on the titers at each time point and the pass 2 virus growth kinetics were not significant (P< .05) even though it had much higher titers than passage 9 and passage 51 viruses at all time points. (These experiments are currently being repeated to further confirm these data).

DISCUSSION

In this study, we examined the sequence differences in a single isolate of FCoV at different passage levels in A-72 canine cells, which were derived from a tumor and are fibroblastic in nature (1). Cats acquire FIPV either by mutations that occur in an endogenous FECV or by infection with exogenous FIPV or both. To help elucidate the origin of FIPV, we examined the genetic differences and growth kinetics of FCoV at different passage levels in cell culture to provide information regarding the capacity of this virus to change.

Sequence analysis of FIPV WSU 79-1146 at passage 1, 8, and 50 showed little or no change in some of the genes. We expected to see most of the changes in spike since that protein is involved in cell attachment and entry into the host cell. However, no differences were maintained between pass 1 and pass 50 and only 1 change R132E was observed between pass 50 and pass 100 in the S glycoprotein.

It has previously been identified that the carboxy terminal domain of the S glycoprotein of FIPV is responsible for more efficient macrophage infection (8). This was identified by exchanging genetic regions from FECV 79-1683 and FIPV 79-1146, two isogenic viruses containing chimeric S glycoproteins one: a FIPV background with a S glycoprotein that had the N-terminal 873 amino acids derived from FECV and the C-terminal 582 amino acids from FIPV and two: a reciprocal hybrid spike gene construct in the FIPV background (8). Both of these recombinants had similar growth kinetics however, only the FIPV recombinant with the C-terminal portion from FIPV 79-1146 was able to readily infect macrophages. The FIPV recombinant with the FECV C-

terminal S protein had a reduced ability to infect macrophages with less than 2% infected cells at 10 hours post infection (8).

It has been shown that the group specific genes, 3abc or 7ab, are associated with virulence in FIPV (5). Thus, it is likely based on our data and previous reports that the development of FIPV is polygenic involving the spike glycoprotein and group specific genes such as 3C and 7b. The 3C gene had the most amino acid differences of all the structural and accessory proteins sequenced in this study. Protein 3C was also truncated to a 165 amino acid protein in all three passages sequenced in this study, when compared to the previously reported 238 amino acid 3C protein in FECV (2). The FCoV accessory protein 3C is a membrane-spanning protein that is predicted to have similar topology to SARS-CoV 3A (10). The SARS-CoV 3A protein is the largest of all accessory proteins at 274 amino acids. This protein localizes to the Golgi, the plasma membrane and intracellular vesicles (4). One study investigated the function of 3A and found that it contributes to the cytotoxicity of SARS-CoV and causes intracellular vesicle formation, which is thought to be necessary for Golgi fragmentation during virus infection (3). However, the depletion of SARS-CoV 3A did not reduce the levels of RNA isolated from infected cells or media indicating this protein and double membrane vesicles may not be necessary for replication (3). Another possibility is that this protein functions to rearrange the Golgi for nonlytic release of virus particles. Such is the case with Poliovirus, which has been identified as using intracellular vesicles and double membrane vesicles for nonlytic release of virus particles (8). The entire 3abc group specific gene cluster has been deleted from FIPV 79-1146 virus, resulting in no significant difference in viral growth in culture but the virus was shown to be attenuated and immunogenic in cats (6).

Upon comparison with the Alphacoronavirus FCoV RM strain, which causes an enteric infection, the FIPV WSU 79-1146 differed in the S glycoprotein and the 3abc genes more than any other region of the genome. While no direct correlation can be made from this comparison because of the lack of information on relationship between the two viruses it is interesting to note that the same two open reading frames have been identified in a genome comparison to have the majority of differences in the Ferret Enteric Coronavirus (FEC) and the Ferret Systemic Coronavirus (12). Both of these

viruses cause similar diseases to FCoV and FIPV respectively, but in ferrets (12). Another example of two closely related CoV that have different tissue cell tropism in the same host resulting in a different disease is the Transmissible Gastroenteritis Virus (TGEV) and the Porcine Respiratory Coronavirus (PRCV). Transmissible Gastroenteritis Virus was indentified in 1946, as the causative agent of a fatal diarrheal disease in neonatal pigs. This virus infects and ultimately destroys the small intestinal enterocytes that are necessary for nutrient absorption and fluid regulation (9). While TGEV has been identified as replicating in the porcine respiratory tract, it does not cause disease. A variant of TGEV was identified in 1983, PRCV, which is antigenically very similar to TGEV yet it replicates much more extensively in the respiratory tract (11). A small deletion in the 1a polyprotein, a 681 nucleotide deletion in the S glycoprotein on the N-terminal, and a truncated ORF 3 have been identified in the comparison between TGEC and PRCV based on transcriptional patterns (11).

We found no apparent adaptation to cell culture based on the growth kinetics of the viruses between tissue passage levels 9 and 51. It was interesting that the first passage in cell culture resulted in a significantly higher titer than subsequent passages. It is not clear why we obtained this result. Since no difference in titer occurred between pass 9 and 51 it will be important to reevaluate the growth curve analysis for the first passage. It has been reported in porcine reproductive and respiratory syndrome virus (PRRSV) that viral load has a direct effect on pathogenicity and immunological responses (7).

Our data indicates that little or no change occur genetically or biologically (growth kinetics) in FCoV following passage in canine A-72 cells indicating that the virus is relatively stable. However, because different selection pressures occur *in vitro* and *in vivo*, it is still unclear if FIPV arises from point mutations that occur during the FECV infection or if they are two closely related circulating viruses or if both of these factors play a role in FIP.

References

- 1. Binn, L. N., R. H. Marchwicki, and E. H. Stephenson. 1980. Establishment of a canine cell line: derivation, characterization, and viral spectrum. Am J Vet Res 41:855-60.
- 2. Chang, H. W., R. J. de Groot, H. F. Egberink, and P. J. Rottier. 2010. Feline infectious peritonitis: insights into feline coronavirus pathobiogenesis and epidemiology based on genetic analysis of the viral 3c gene. J Gen Virol 91:415-20.
- 3. Freundt, E. C., L. Yu, C. S. Goldsmith, S. Welsh, A. Cheng, B. Yount, W. Liu, M. B. Frieman, U. J. Buchholz, G. R. Screaton, J. Lippincott-Schwartz, S. R. Zaki, X. N. Xu, R. S. Baric, K. Subbarao, and M. J. Lenardo. 2010. The open reading frame 3a protein of severe acute respiratory syndrome-associated coronavirus promotes membrane rearrangement and cell death. J Virol 84:1097-109.
- 4. Freundt, E. C., L. Yu, E. Park, M. J. Lenardo, and X. N. Xu. 2009. Molecular determinants for subcellular localization of the severe acute respiratory syndrome coronavirus open reading frame 3b protein. J Virol 83:6631-40.
- 5. Haijema, B. J., H. Volders, and P. J. Rottier. 2004. Live, attenuated coronavirus vaccines through the directed deletion of group-specific genes provide protection against feline infectious peritonitis. J Virol 78:3863-71.
- 6. Haijema, B. J., H. Volders, and P. J. Rottier. 2003. Switching species tropism: an effective way to manipulate the feline coronavirus genome. J Virol 77:4528-38.
- 7. Johnson, W., M. Roof, E. Vaughn, J. Christopher-Hennings, C. R. Johnson, and M. P. Murtaugh. 2004. Pathogenic and humoral immune responses to porcine reproductive and respiratory syndrome virus (PRRSV) are related to viral load in acute infection. Vet Immunol Immunopathol 102:233-47.
- 8. Kirkegaard, K., and W. T. Jackson. 2005. Topology of double-membraned vesicles and the opportunity for non-lytic release of cytoplasm. Autophagy 1:182-4.
- 9. Moon, H. W. 1978. Mechanisms in the pathogenesis of diarrhea: a review. J Am Vet Med Assoc 172:443-8.
- 10. Oostra, M., E. G. te Lintelo, M. Deijs, M. H. Verheije, P. J. Rottier, and C. A. de Haan. 2007. Localization and membrane topology of coronavirus nonstructural protein 4: involvement of the early secretory pathway in replication. J Virol 81:12323-36.
- 11. Wesley, R. D., R. D. Woods, and A. K. Cheung. 1991. Genetic analysis of porcine respiratory coronavirus, an attenuated variant of transmissible gastroenteritis virus. J Virol 65:3369-73.
- 12. Wise, A. G., M. Kiupel, and R. K. Maes. 2006. Molecular characterization of a novel coronavirus associated with epizootic catarrhal enteritis (ECE) in ferrets. Virology 349:164-74.

Table 4.1. Nonstructural proteins in ORF 1a and 1ab locations and changes that occurred between passages of the virus in Feline Coronavirus 79-1146 passage 1, passage 8, and passage 50.

D:00	FII	PV WSU7	9-1146:Pass1	Pass8	Pass50	Pass100*	Total A.A
Diff.	Cleavage Site	Size					
Nsp 1	1Met-Gly110	110	-	-	-	-	0
Nsp 2	111Ala- Gly879	769	177-D 388-W 807-K	177-G 388-W 807-K	177-G 388-C 807-K	177-G 388-C 807-T	3
Nsp 3	880Gly- Gly2413	1534	1784-A	1784-A	1784-A	1784-V	1
Nsp 4	2414Ser- Gln2903	490	2888-M	2888-M	2888-M	2888-K	1
Nsp 5	2904Ser- Gln3205	302	2909-M 2936-G	2909-M 2936-G	2909-I 2936-R	2909-M 2936-G	2
Nsp 6	3206Ser- Gln3499	294	3280-A	3280-A	3280-A	3280-V	1
Nsp 7	3500Ser-3582- Gln	83	3558-F 3571-I	3558-C 3571-M	3558-F 3571-I	3558-F 3571-I	2
Nsp 8	3583Ser- Gln3777	195	3606-E 3607-A 3618-K	3606-A 3607-G 3618-N	3606-E 3607-A 3618-K	3606-E 3607-A 3618-K	3
Nsp 9	3778Asn- Gln3888	111	3805-G 3840-I 3860-V	3805-A 3840-N 3860-G	3805-G 3840-I 3860-V	3805-G 3840-I 3860-V	3
Nsp 10	3889Ala- Gln4023	135	3992-Q	3992-Q	3992-Q	3992-R	1
Nsp 11	4024Gly- Asp4047	19	-	-	-	-	0
Nsp 12	4024Gly- Gln4952	929	4707-T 4708-A	4707-I 4708-A	4707-T 4708-C	4707-T 4708-A	2
Nsp 13	4953Ala- Gln5551	599	5050-D	5050-V	5050-V	5050-V	1
Nsp 14	5552Ala- Gln6070	519	5846-Y	5846-Y	5846-Y	5846-Н	1
Nsp 15	6071Ser- Gln6409	339	-	-	-	-	0
Nsp 16	6410Ser- 6709Pro	300	-	-	-	-	0

^{*} FIPV WSU 79-1146 p100 was not sequenced in our laboratory (Dye and Siddell, 2005).

Table 4.2. Location of open reading frames, size of protein, and differences that occurred in passages of the virus in Feline Coronavirus 79-1146, pass 8, and pass 50. Abbreviations: S-Spike glycoprotein, 3a-3a accessory protein, 3b- 3b accessory protein, 3c-3c accessory protein, E-Small envelope protein, M-membrane, N-Nucleocapsid, 7a-7a accessory protein, and 7b accessory protein. All numbers correspond to the Orf's individually

ORF nucleotide position	Translation product (amino acids)	Amino Acid Identity Differences WSU 791146			
		Pass0	pass8	pass50 pa	ss100**
Orf 1a 311-12439	Polyproteins 1a (4042)	See table	1		
Orf 1ab 311-20439	Polyprotein 1ab (6653)	See table	1		
Orf S 20436-24794	Spike glycoprotein (1452)	599-T 743-A 1325R	599-A 743-A 1325R	599-T 743-A 1325R	599-T 743-V 1325E
Orf 3a 24861-25076	Accessory protein 3a (71)	61-F	61-S	61-F	61-F
Orf 3b 25021-25236	Accessory protein 3b (71)	-	-		-
Orf 3c 25470-25967	Accessory protein 3c (165)	25-V 35-F 42-Y 52-N	25-G 35-F 42-I 52-H	25-V 35-L 42-Y 52-N	25-V* 35-L* 42-Y* 52-N*
Orf E 25954-26202	Small Membrane Protein (82)	71-I	71-T	71-T	71-T
Orf M 26213-27001	Membrane protein (262)	-	-	-	-
Orf N 27014-28147	Nucleocapsid protein (377)	18-L	18-L	18-L	18-R
Orf 7a 28131-28457	Accessory protein 7a (108)	39-L	39-L	39-L	39-M
Orf 7b 28462-29082	Accessory protein 7b (206)	-	- trun	cated @ 48 A.A trun	cated @ 48 A.A

^{*}Indicates that amino acid position is not consistent with previous passages due to a rearrangement see figure 4. ** FIPV WSU 79-1146 p100 was not sequenced in our laboratory (Dye and Siddell, 2005).

Table 4.3. List of Coronavirus isolates and strains included in the sequence and phylogenetic analysis.

No.	Isolate/Strain	Accession No.	Origin	Reference
1	FCoV/UU11/Netherlands/2007	FJ938052.1	Netherlands	Direct
				submission
2	FCoV/UU10/Netherlands/2007	FJ938059.1	Netherlands	Direct
		EX020062 1	37.1.1.1	submission
3	FCoV/UU9/Netherlands/2007	FJ938062.1	Netherlands	Direct
4	FC-V/III54/N-dd1-/2010	D1102002 1	N1-4111-	submission
4	FCoV/UU54/Netherlands/2010	JN183883.1	Netherlands	Direct
5	FCoV/UU30/Netherlands/2008	HQ392472.1	Netherlands	submission Direct
3	red v/0030/Netherlands/2008	11Q392472.1	inculcitatios	submission
6	FCoV/UU2/California/1993	FJ938060.1	California	Direct
	1 00 1/0 02/04/10/11/4/1999	13730000.1	Cumoma	submission
7	FCoV/FECV/Black/1970	EU186072.1	US	Tekes,G.,et al.,
,	1 66 (/1 26 (/2 west 15 / 6	20100072.1		2008
8	FCoV/UU47/Netherlands/2010	JN183882	Netherlands	Town,C.D.,et
				al., 2011
9	FCoV/UU16/Netherlands/2007	FJ938058.1	Netherlands	Spiro,D.,et al.,
				2009
10	FCoV/FIPVC1JE	DQ848678.1	-	Dye & Siddell,
				2006
11	FCoV/FIPV WSU 79-1146/p8	*	-	-
12	FCoV/FIPVWSU79-1146/p50	*	-	
12	FO M/FIDMMONIZO1146/NICA	D0010021	TICA	- 0.0:11.11
13	FCoV/FIPVWSU791146/USA	DQ010921	USA	Dye&Siddell
14	FCoV/FIPV WSU 79-1146/p1	*	-	
14	reov/rii v wso /9-1140/pi		-	-
15	FCoV/DF-2/USA	DQ286389.1	US	Direct
	2 2 2 7 7 2 2 2 2 2 2 2 2 2 2 2 2 2 2 2	_ <		Submission
16	FCoV/FECV/WSU79-1683	*	-	Direct
				submission
17	TGeV/Purdue/Pur46-Mad	NC_002306.2		Almazan,F.,et
				al., 2001
18	TGeV/Purdue/P126	DQ811788.1	USA	Spiro et al.,
				2006
19	CCoV/NTU336/F/2008	GQ477367	Taiwan	Direct
20		00150141	T	submission
20	FCoV/NTU156/p/2007	GQ152141	Taiwan	Direct
21	WBCoV/US/OH-WD358-TC/1994	E1425104.1	US	submission
21	WBC0V/US/OH-WD358-1C/1994	FJ425184.1	US	Spiro,D., et al., 2008
22	SDCoV/US/OH-WD-388-TC/1994	FJ425188.1	US	Spiro,D., et al.,
22	3DC0 V/OS/O11-W D-388-1C/1994	13423100.1	US	2008
23	HCoV/4408/Germany/1988	FJ415324	Germany	Zhu,H.,et al.,
23	1100 1/1100/Germany/1700	10110027	Germany	2008
24	SaCoV/US/OH1/2003	EF424621.1	US	Zhang,X.,et al.,
				2007
	· · · · · · · · · · · · · · · · · · ·	· · · · · · · · · · · · · · · · · · ·		

25	GCoV/US/OH3-TC/2006	EF424622.1	US	Hasoksuz,M.,et al., 2007
26	CGCoV/US/OH3/2006	EF424624.1	US	Hasoksuz,M.,et al., 2007
27	EqCoV/NC99	EF446615.1	-	Zhang,J.,et al., 2007
28	BatCoV/AFCD62/HongKong	NC_010437.1	China	Chu,D.K., et al., 2008
29	TGeV/SC-V/China	DQ443743	China	Direct submission
30	TGeV/TGeVMiller16/16	DQ811785.1	-	Zhang,X.,et al., 2007
31	PRCV/PRCVISu-1/18	DQ811787.1	-	Zhang,X.,et al., 2007

^{*}Indicates Virus sequenced in Jackwood Lab accession numbers have not been given yet.

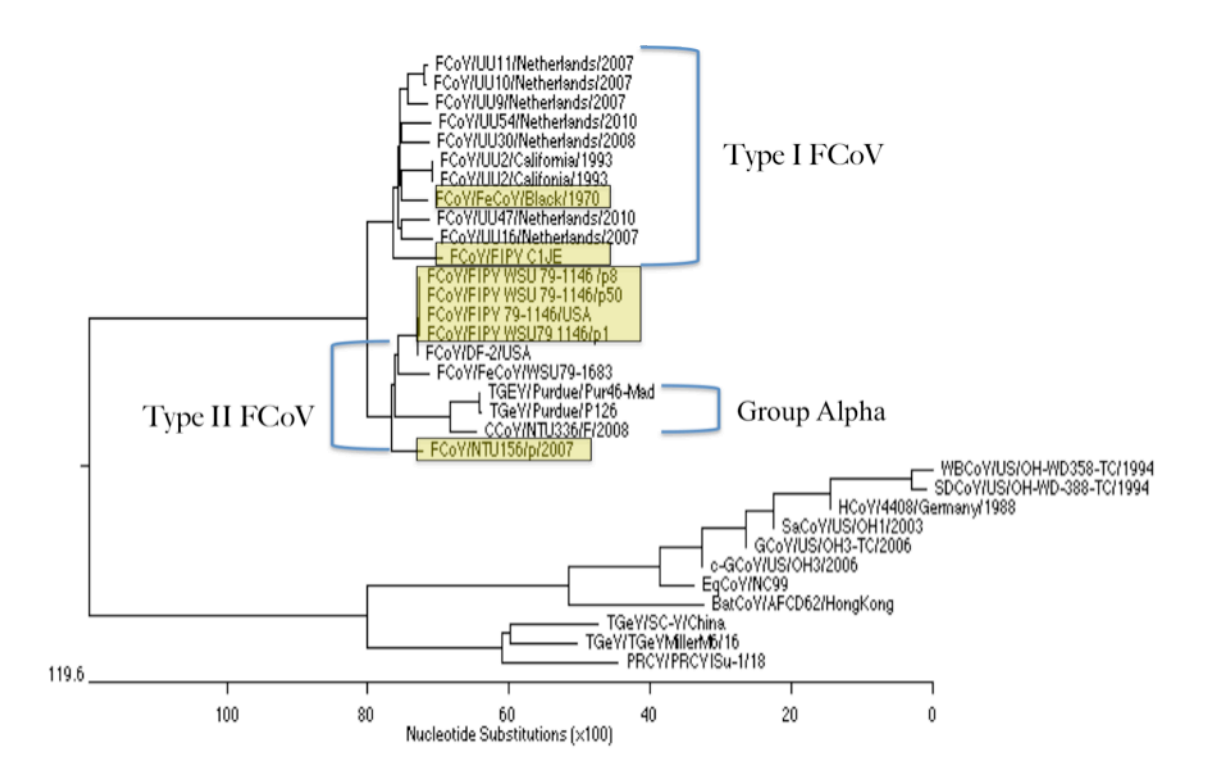


Figure 4.1. Neighbor-Joining method used to infer evolutionary history using full genomic sequence data of the available Feline CoV. The FCoV that are identified as FIPV have been highlighted in yellow. The bootstrap consensus tree was constructed from 1000 replicates (percentage of replicate trees in which associated strains clustered together are presented at nodes).

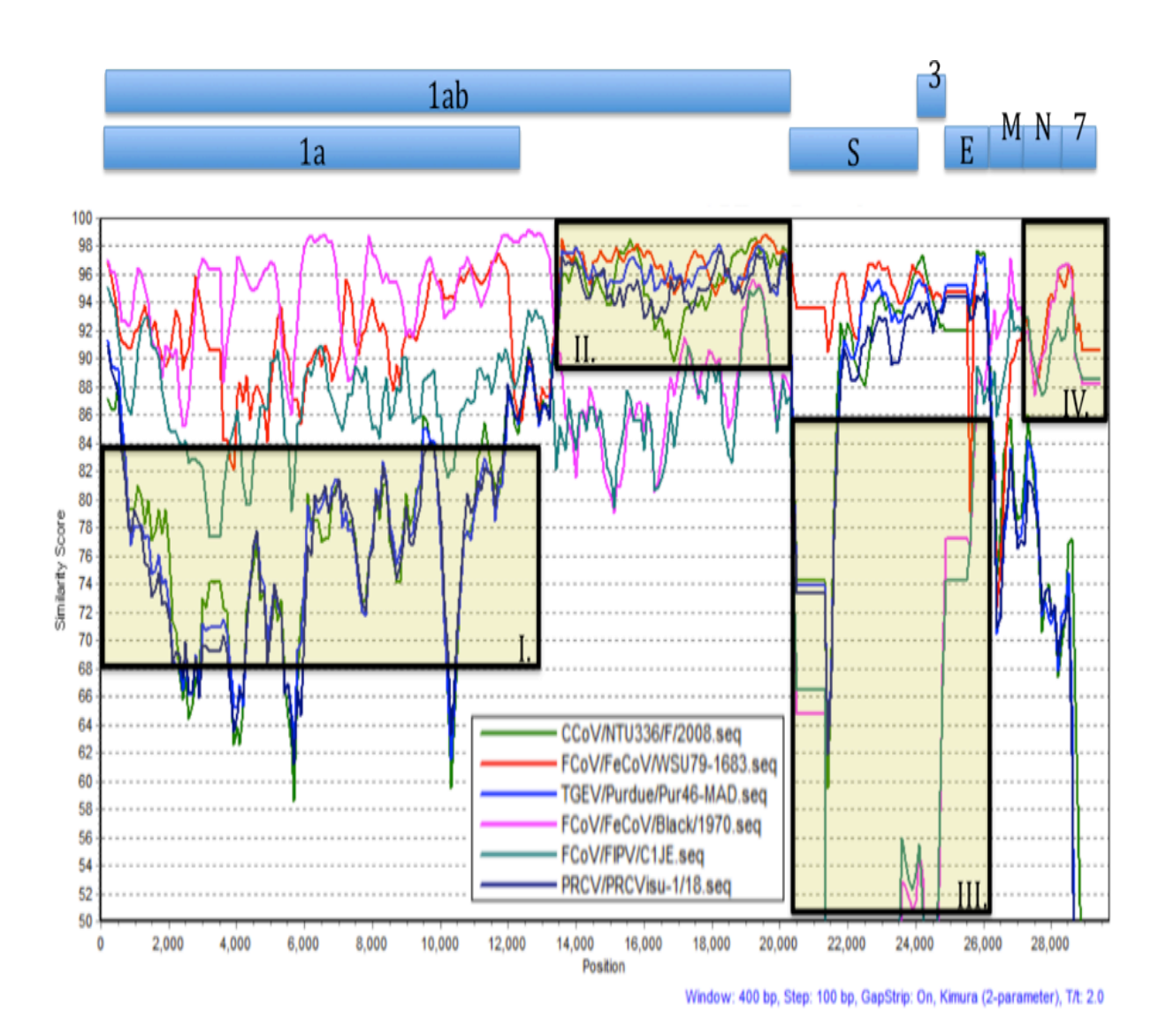
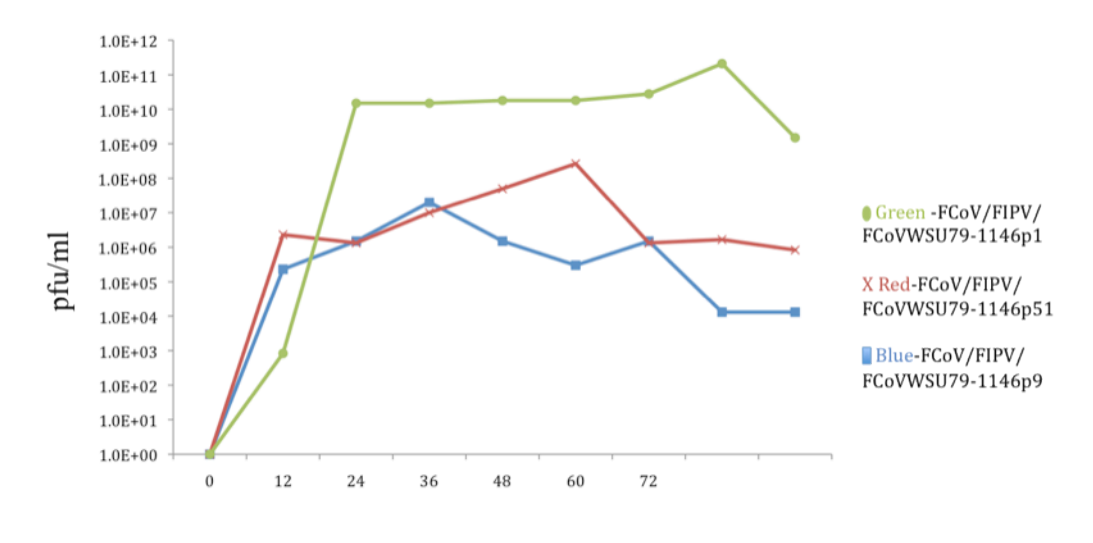


Figure 4.2. Simplot analysis of full-length genomic sequence for CCoV/NTU336/F/2008, FCoV/FECV/79-1683, TGEV/Purdue/Pur46-MAD, FCoV/FIPV/C1JE, and PRCV/PRCVisu-1/18 showing recombination between nucleotides ~14,000-20,000. The query sequence is FCoV/FIPV/FCoVWSU79-1146pass1. Bars at the top represent relative position of the coding regions for 1a, 1ab, spike, gene 3abc (3), envelope (E), membrane (M), nucleocapsid (N), and genes 7a/b (7).



Time (hours) post infection

Figure 4.3. Growth curve analysis of FIPV WSU79-1146 isolates at different tissue passage levels in A72, performed in triplicate. A72 Canine Kidney Cells were infected at a MOI of 0.1.

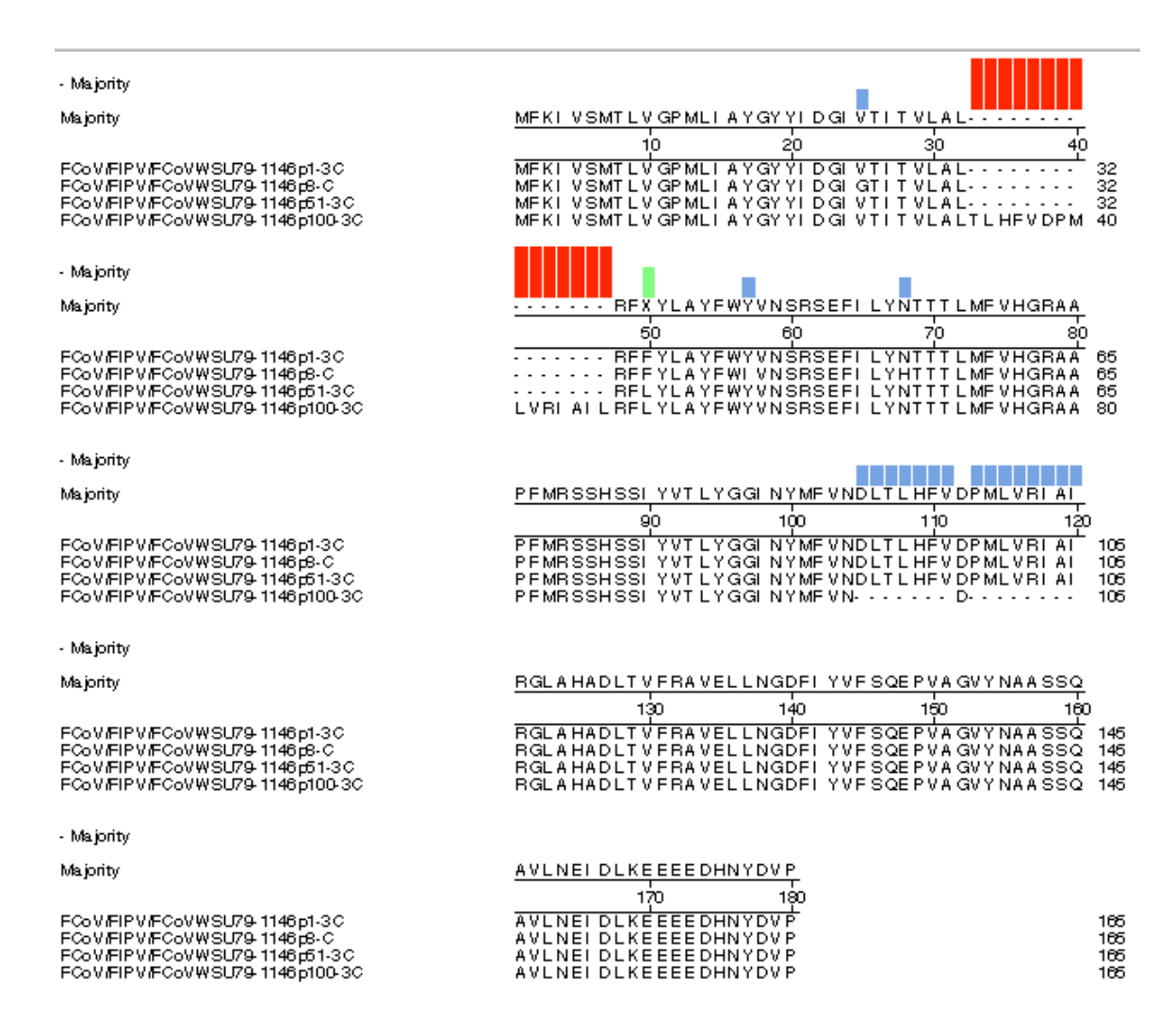


Figure 4.4. Three C protein alignment of FCoV/FIPV/FCoVWSU79-1146 at passage 1, 8, 51, and p100. Alignment created using Clustal W in Megalign Laser Gene.

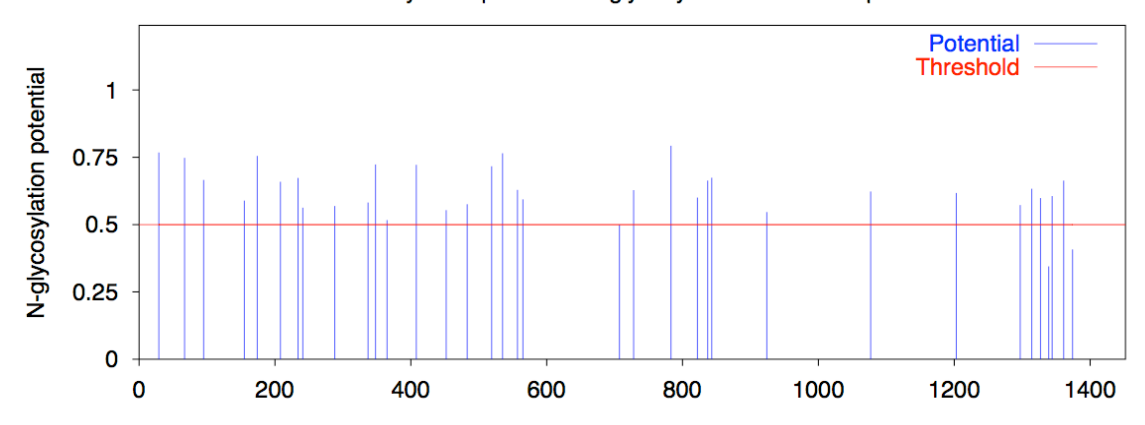


Figure 4.5. An illustration of potential N-glycosylation sites in the Spike protein of FCoV/FIPVWSU79-1146 p50. The graph illustrates predicted N-glyc sites across the protein chain (x-axis represents protein length from N- to C-terminal). A position with a potential (vertical lines) crossing the threshold (horizontal line at 0.5) is predicted glycosylated. (http://www.cbs.dtu.dk).

CHAPTER 5

TRANSMISSION DYNAMICS OF GAMMACORONAVIURS INFECTIOUS BRONCHITIS VIRUS $^{\rm 3}$

³ Phillips, J.E., Hilt, D.A., and Jackwood, M.W. To be submitted to *Avian Pathology*

ABSTRACT

Infectious bronchitis virus (IBV) can be found worldwide, and is rapidly transmitted among poultry of all ages. Selection working on mutations and recombination events as the virus replicates and is transmitted within a population results in evolution of the virus. However, transmission as it relates to the dynamics of viral evolution has not been extensively studied in the natural host. In this study, we conducted a chain of transmission experiment and measured the viral load, the infectious period, and the latent period. A founder nine-day-old chicken was infected with the Arkansas-DPI strain of IBV and allowed to naturally transmit the virus to contact control birds. The first contact control bird to become infected was moved to a separate isolator and mixed with other susceptible birds, and in this way the chain of transmission was maintained for 10 events. The spike glycoprotein gene of the virus in the inoculum, the virus isolated in transmission 3, and the virus isolated in transmission 10 was sequenced and surprisingly, no nucleotide changes were observed in the consensus sequences. Viral clearance was more rapid during later transmissions and the average latent period decreased significantly after the third transmission event. This data indicates that the virus is adapting to the host but that adaptation is not reflected in the spike gene sequence. This information is important in understanding the dynamics of viral evolution as it relates to transmission and hopefully can be used to better control this important disease in poultry in the future.

INTRODUCTION

Infectious Bronchitis Virus (IBV) causes an upper respiratory tract disease in poultry as well as predisposes birds to secondary bacterial infections. Live attenuated vaccines are used to control the disease however; little cross-protection occurs between different serotypes of the virus. Since the discovery of the Massachusetts strain in the 1930s, numerous serotypes have been identified thus making the disease difficult to control. The spike (S) glycoprotein is responsible for mediating virus attachment to the host cell, it contains neutralizing epitopes, and hypervariable regions (HVR), which determine the serotype of the virus.

Infectious bronchitis virus exists as genetically diverse populations of related virus particles (7, 12, 13). It has previously been shown that the S glycoprotein undergoes selection in the host during infection resulting in the accumulation of nucleotide changes (8). It has also been shown that multiple subpopulations within the same serotype exist for each virus (12). Viral subpopulations in IBV are believed to be a result; of infidelity of the RNA-dependent RNA polymerase, replication by a "copy choice mechanism" that leads to homologous recombination, and the virus's large genome size, which gives coronaviruses extra plasticity (15). Several studies have examined evolutionary principals such as the dynamics of adaptation, recovery from deleterious mutations, evolution of mutational robustness, mutational load, transmission bottlenecks and Muller's ratchet, evolution of competitive interactions and more (6). Although, these studies gave great insight into the mechanism of viral evolution, most of them did not study the virus as it is transmitted in a natural infection from host to host (2, 4, 9, 14).

In a completely susceptible population of individuals the expected average number of new cases caused by a virus, is defined as the reproductive number (R_0) . This number is based on four parameters: infectious period, probability of transmission, probability that a new case is infectious, and the number of infectious contacts. If R_0 is less than one the disease will not be sustained. An R_0 value equal to one indicates the number of individuals with disease will remain steady in the population and if it is greater than one the disease will spread resulting in an epidemic. While R_0 is a good indicator of the virus's ability to spread in a population, it can be manipulated. Vaccination is one way to

alter the R_0 value because vaccination reduces the number of susceptible individuals in a population. One study evaluated the transmission of IBV within vaccinated and unvaccinated groups of chickens and found that a single homologous vaccination reduced IBV transmission compared to unvaccinated birds with R_0 equal to 0.69 and 19.95 respectively (5).

In order to look at transmission and subsequent amplification of the virus in the host plays on the selection of virus subpopulations, we conducted a natural chain of transmission study where IBV was transmitted ten times in its natural host, the chicken. We examined viral load, the infectious period, the latent period, and nucleotide changes in the S glycoprotein at various transmission events to better understand the dynamics of viral evolution in its natural host.

MATERIAL AND METHODS

Animals

One-day-old specific pathogen free chicks were obtained from Merial (Gainesville, GA) and birds were housed in positive pressure HEPA filtered Horsfal isolation units. Feed and water were given *ad libitum*.

Inoculum

We initially infected a single bird (designated Inf-1) at nine days of age with 1 X 10^4 50% embryo infectious doses (EID₅₀) of the Ark/Ark-DPI p8/91 pathogenic virus by the intranasal/intraocular route, which is the natural route of infection for IBV.

Transmission experiment

A chain of transmission experiment was conducted wherein 10 natural transmission events were monitored. The onset of virus shedding was measured by

collecting intrachoanal and tracheal swabs approximately every 12 hours, beginning 12 hours after infection, to avoid detection of the inoculum. The samples were then immediately tested by real time RT-PCR. As soon as virus was detected in the founder bird, 2 susceptible contact birds were placed in the isolation unit. When virus was detected in one of the contact birds, it was immediately removed from the group and placed in a separate isolator to avoid transmission between contact birds. The initial virus positive contact bird (designated Inf-2) was then used to continue the chain of transmission. Two susceptible contact birds were immediately placed in a separate isolator with the Inf-2 bird and monitored for virus by real time RT-PCR. In this manner, the chain of transmission was continued for 10 transmission events.

Trachea vs. choanal cleft swabs

In this study, we also compared the amount of virus detected in the trachea versus the choanal cleft to determine if choanal cleft swabbing correlated with swabbing the trachea. Both the trachea and choanal cleft for all of the birds in the chain of transmission experiment, described above, were swabbed every twelve hours until identified as no longer positive for virus by real-time PCR.

RNA extraction and real-time RT-PCR assay

Extraction of RNA from trachea and choanal swab samples was performed using the MagMax 96 Total RNA isolation kit (Ambion, Austin, TX) following the manufacturer's suggestions. The RNA was used as template in the real-time RT-PCR assay as previously described (3), and the cycle threshold (CT) value was used to calculate the genome copy number.

Spike gene amplification and sequencing

Amplification of the S1 portion of the spike gene by RT-PCR was performed using the Titan one tube RT-PCR kit (Roche Diagnostics) according to manufacturers

protocol with primers NEWS1oligo5' and S1 degenerate 3' as previously described (10). The amplified products were purified and cycle sequencing was conducted using the BigDye Terminator v3.1 Cycle Sequencing Kit (Applied Biosystems, Foster City, Ca). The sequencing reactions were run on an ABI 3730 sequencer (Applied Biosystems, Foster City, CA) at the Molecular Genetics Instrumentation Facility (University of Georgia, Athens, GA). The S1 gene sequences were analyzed using EditSeq and MegAlign (DNASTAR Inc., Madison, WI) and by Finch TV (Geospiza, Inc., Seattle, WA).

Statistical analysis

The data were analyzed using the statistical software program Jump (MP, Version 7. SAS Institute Inc., Cary, NC).

RESULTS

Virus detection in tracheal and choanal cleft swabs

No statistical difference (Students T-test p<0.9676) was found in the viral genome copy number between paired samples (from the same bird) of tracheal and choanal cleft swabs (Figure 1).

Transmission dynamics

Infectious Bronchitis Virus strain Ark/Ark-DPI p8/91 was successfully transmitted a total of 10 times in SPF chicks (Figure 2). Our results showed that IBV is more rapidly transmitted among chicks after the third transmission event (Figure 3). The latent period was 66 hours for the first transmission event, 96 hours for the second transmission event and 33.7 hours for the third transmission event. Interestingly, clearance of the virus or the infectious period was as high as 336 hours (14 days) for early transmission events and as short as 168 hours (7 days) for the later transmission

events (Figure 4). The peak viral load for all twenty-one birds, occurred at 6.5 days with an average of 1 \times 10^{5.379} per sample, calculated from CT values as previously performed (3). The maximum level of viral load in each bird did not appear to correlate with time of viral clearance (Figure 6).

Sequencing the S1 gene

No nucleotide changes were identified in the consensus sequences of the first 1600 nucleotides of the S glycoprotein gene from the inoculum, transmission event number 3, and 10 (Figure 6). However, a few minor peaks were identified in the sequence indicating the presence of subpopulations. These minor peaks need to be investigated further to confirm that they are not sequencing artifacts.

DISCUSSION

We conducted a chain of natural transmission with IBV in chickens to analyze transmission dynamics of the virus. A comparison was made with viral RNA isolated from the trachea and the choanal cleft, at the same time point from the same bird. No statistical difference was found in the amount of viral genome detected from the trachea vs. the choanal cleft. We examined this correlation because swabbing the choanal cleft is much easier and less invasive than swabbing the trachea. Thus, this technique can be used for virus detection without compromising the epithelium in the trachea.

Our results indicate that IBV is more rapidly transmitted among chickens after the first three transmission events. The peak viral load during infection occurred at six and a half days, which is similar to what was previously reported for IBV (3). Callison *et al.* reported that maximum viral load was reached within five days post infection (3). In addition, we found that the infectious period became shorter in the later transmission events.

No nucleotide changes were detected in the S glycoprotein gene consensus sequence, although minor peaks were present in the sequence of viruses isolated in the

later transmission events. Shortening of the latent period suggests that the virus is adapting to the host, however; no sequence changes in the S1 gene indicates that mutations are occurring in other genes. A previous study showed that the pathogenicity genes are located in the 1a/ab region of the viral genome which encodes the viral replication complex (1). It is possible that genetic changes affecting latent period may have occurred in that region.

The infectious period shortened from the first bird being positive for over 300 hours to below 200 hours for the bird in the tenth transmission event. The first birds were 9-days old at the time of infection, whereas the contact birds in the tenth transmission event were 29 days old. The maturity of the birds by the tenth transmission realistically reflects the age of the birds in the field, but it is possible that the age of the birds in the later transmission events could account for the more rapid viral clearance due to a more developed immune system. Matthijis et al. reported that broilers infected with IBV M41, at 15 days of age were able to clear the virus within 13-15 days which was significantly faster than what they found at day 1 of age (11). They speculated that older birds have a more-efficient clearance mechanism due to a maturation of the immune system. Our results coincide with these findings and suggest that R0 may decrease as birds mature (5).

Elucidating the transmission dynamics of IBV is important for understanding how the virus is maintained in a population of chickens. Gaining a more detailed picture of the natural transmission of IBV among chickens is also important for developing effective control strategies.

References

- 1. Armesto, M., D. Cavanagh, and P. Britton. 2009. The replicase gene of avian coronavirus infectious bronchitis virus is a determinant of pathogenicity. PLoS One 4:e7384.
- 2. Bouma, A., I. Claassen, K. Natih, D. Klinkenberg, C. A. Donnelly, G. Koch, and M. van Boven. 2009. Estimation of transmission parameters of H5N1 avian influenza virus in chickens. PLoS Pathog 5:e1000281.
- 3. Callison, S. A., D. A. Hilt, T. O. Boynton, B. F. Sample, R. Robison, D. E. Swayne, and M. W. Jackwood. 2006. Development and evaluation of a real-time Taqman RT-PCR assay for the detection of infectious bronchitis virus from infected chickens. J Virol Methods 138:60-5.
- 4. Coffey, L. L., N. Vasilakis, A. C. Brault, A. M. Powers, F. Tripet, and S. C. Weaver. 2008. Arbovirus evolution in vivo is constrained by host alternation. Proc Natl Acad Sci U S A 105:6970-5.
- 5. de Wit, J. J., M. C. de Jong, A. Pijpers, and J. H. Verheijden. 1998. Transmission of infectious bronchitis virus within vaccinated and unvaccinated groups of chickens. Avian Pathol 27:464-71.
- 6. Elena, S. F., and R. Sanjuan. 2007. Virus evolution: Insights from an experimental approach. Annual Review of Ecology Evolution and Systematics 38:27-52.
- 7. Gallardo, R. A., F. J. Hoerr, W. D. Berry, V. L. van Santen, and H. Toro. 2011. Infectious bronchitis virus in testicles and venereal transmission. Avian Dis 55:255-8.
- 8. Gallardo, R. A., V. L. van Santen, and H. Toro. 2010. Host intraspatial selection of infectious bronchitis virus populations. Avian Dis 54:807-13.
- 9. Hoelzer, K., P. R. Murcia, G. J. Baillie, J. L. Wood, S. M. Metzger, N. Osterrieder, E. J. Dubovi, E. C. Holmes, and C. R. Parrish. 2010. Intrahost evolutionary dynamics of canine influenza virus in naive and partially immune dogs. J Virol 84:5329-35.
- 10. Lee, C. W., D. A. Hilt, and M. W. Jackwood. 2003. Typing of field isolates of infectious bronchitis virus based on the sequence of the hypervariable region in the S1 gene. J Vet Diagn Invest 15:344-8.
- 11. Matthijs, M. G., A. Bouma, F. C. Velkers, J. H. van Eck, and J. A. Stegeman. 2008. Transmissibility of infectious bronchitis virus H120 vaccine strain among broilers under experimental conditions. Avian Dis 52:461-6.
- 12. McKinley, E. T., D. A. Hilt, and M. W. Jackwood. 2008. Avian coronavirus infectious bronchitis attenuated live vaccines undergo selection of subpopulations and mutations following vaccination. Vaccine 26:1274-84.
- 13. Nix, W. A., D. S. Troeber, B. F. Kingham, C. L. Keeler, Jr., and J. Gelb, Jr. 2000. Emergence of subtype strains of the Arkansas serotype of infectious bronchitis virus in Delmarva broiler chickens. Avian Dis 44:568-81.
- 14. van der Goot, J. A., G. Koch, M. C. de Jong, and M. van Boven. 2005. Quantification of the effect of vaccination on transmission of avian influenza (H7N7) in chickens. Proc Natl Acad Sci U S A 102:18141-6.

Woo, P. C., S. K. Lau, Y. Huang, and K. Y. Yuen. 2009. Coronavirus diversity, phylogeny and interspecies jumping. Exp Biol Med (Maywood) 234:1117-27.

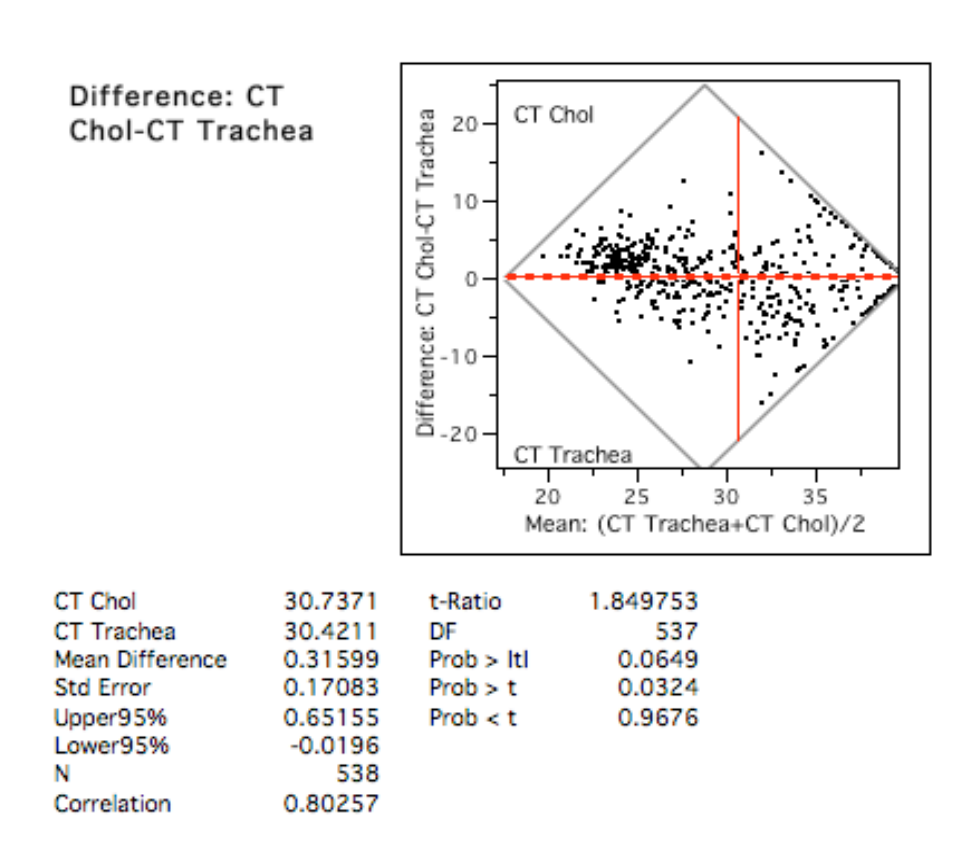


Figure 5.1. Scatter plot of the CT values from tracheal vs. choanul swab. No statistical significance was identified between the two methods for viral isolation.

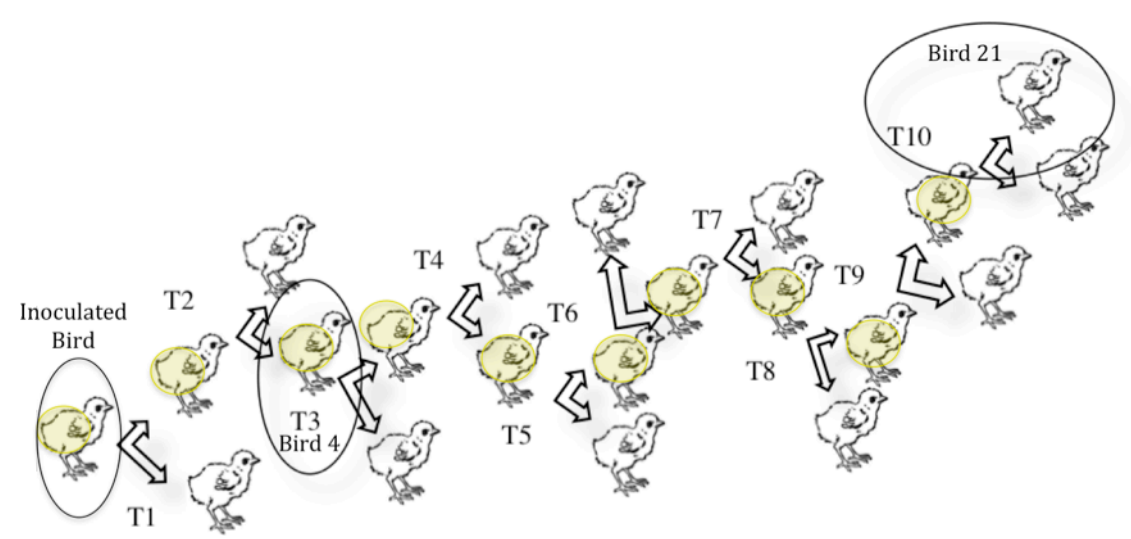


Figure 5.2. Diagram of the natural transmission study. Circles indicate the transmission number and bird where virus was reisolated and S1 was sequenced. Yellow dots indicate the contact bird that was identified as positive first and subsequently used to continue the chain of transmission.

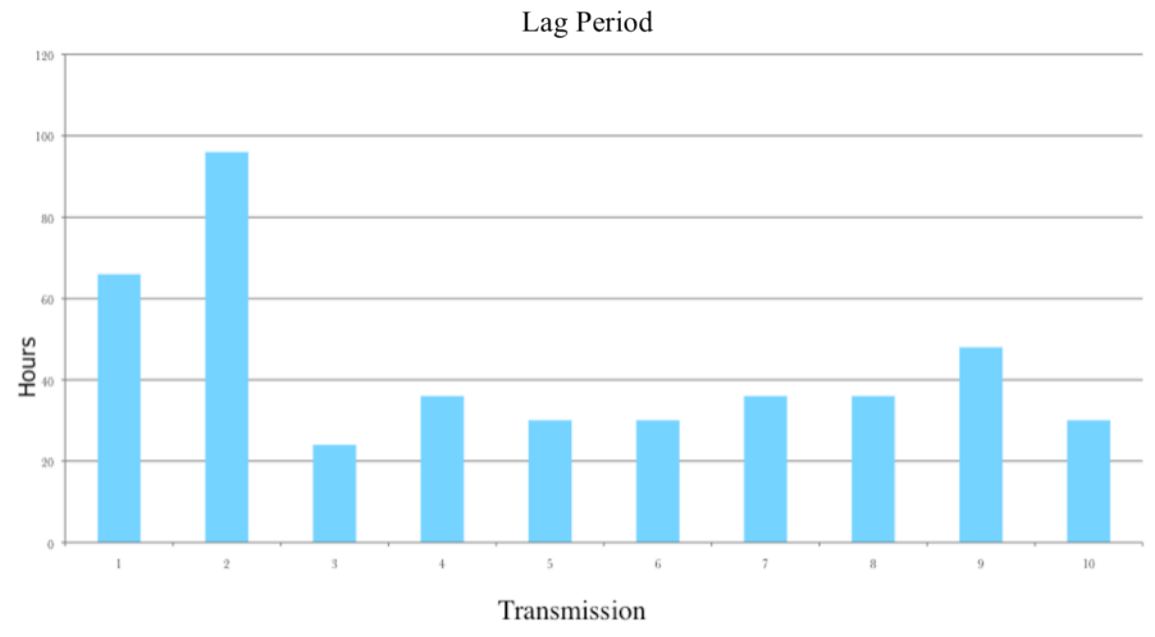


Figure 5.3. The average time (between both contact birds) from infection (exposure from infected contact bird from prior transmission event) to detection of the virus in the bird.

Infectious Period

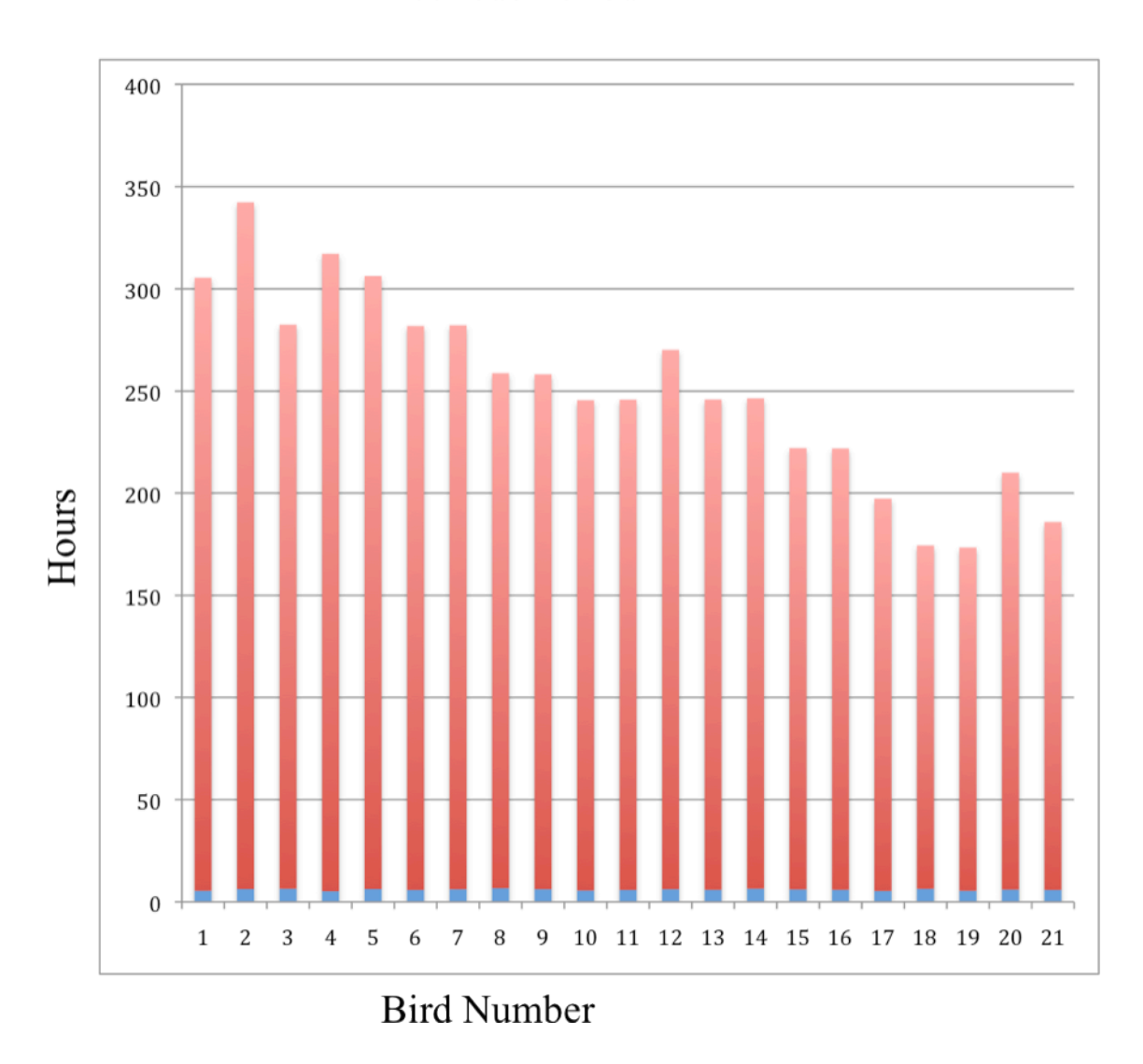


Figure 5.4. The length (hrs.), that the infected birds were identified as positive for virus isolation.

Majority	ATGTTGGTGA AGT CACTGTTTCTAGTGA CC 10 20 30
Ark/Ark-DPI p8/91 inoculum B-4-10 Transmission 3 B-21-12 Transmission 10	ATGTTGGTGAAGTCACTGTTTCTAGTGACC 30 ATGTTGGTGAAGTCACTGTTTCTAGTGACC 30 ATGTTGGTGAAGTCACTGTTTCTAGTGACC 30
- Majority	
Majority	ATTTTGTTTGCACTATGTAGTGCTAATTTA 40 50 60
Ark/Ark-DPI p8/91 inoculum B-4-10 Transmission 3 B-21-12 Transmission 10	ATTTTGTTTGCACTATGTAGTGCTAATTTA 60 ATTTTGTTTGCACTATGTAGTGCTAATTTA 60 ATTTTGTTTGCACTATGTAGTGCTAATTTA 60
- Majority	
Majority	TATGACAACGAATCTTTTGTGTATTACTAC
Ark/Ark-DPI p8/91 inoculum B-4-10 Transmission 3 B-21-12 Transmission 10	70 80 90 TATGACAACGAATCTTTTGTGTATTACTAC 90 TATGACAACGAATCTTTTGTGTATTACTAC 90 TATGACAACGAATCTTTTGTGTATTACTAC 90
- Majority	
Majority	CAGAGTGCTTTAGGCCAGGACATGGTTGG
Ark/Ark-DPI p8/91 inoculum B-4-10 Transmission 3 B-21-12 Transmission 10	100 120 CAGA GT GCTTTTA GGC CAGGA CAT GGTT GG 120 CAGA GT GCTTTTA GGC CAGGA CAT GGTT GG 120 CAGA GT GCTTTTA GGC CAGGA CAT GGTT GG 120
- Majority	
Majority	CATTTACATGGAGGTGCTTATGCAGTAGTT 130 140 150
Ark/Ark-DPI p8/91 inoculum B-4-10 Transmission 3 B-21-12 Transmission 10	CATTTACATGGAGGTGCTTATGCAGTAGTT 150 CATTTACATGGAGGTGCTTATGCAGTAGTT 150 CATTTACATGGAGGTGCTTATGCAGTAGTT 150
Majority	AATGTGTCTAGTGAAAATAATAATGCAGGT 160 170 180
Ark/Ark-DPI p8/91 inoculum B-4-10 Transmission 3 B-21-12 Transmission 10	AATGTGT CTAGTGAAAATAATAATGCAGGT 180 AATGTGT CTAGTGAAAATAATAATGCAGGT 180 AATGTGT CTAGTGAAAATAATAATGCAGGT 180
- Majority	
Majority	ACTGCCCAAGTTGCACTGCTGGTGCTATT 190 200 210
Ark/Ark-DPI p8/91 inoculum B-4-10 Transmission 3 B-21-12 Transmission 10	ACTGCCCAAGTTGCACTGCTGGTGCTATT 210 ACTGCCCCAAGTTGCACTGCTGGTGCTATT 210 ACTGCCCCAAGTTGCACTGCTGGTGCTATT 210
- Majority	
Majority	GGCT A CA GT A A GA A TT T CA GT G C GG C CT CA 220 230 240
Ark/Ark-DPI p8/91 inoculum B-4-10 Transmission 3 B-21-12 Transmission 10	GGCTACAGTAGAATTTCAGTGCGCCCTCA 240 GGCTACAGTAAGAATTTCAGTGCGGCCTCA 240 GGCTACAGTAAGAATTTCAGTGCGGCCTCA 240
- Majority	
Majority	GTAGCCATGACTGCACCACTAAGTGGTATG
Ark/Ark-DPI p8/91 inoculum B-4-10 Transmission 3 B-21-12 Transmission 10	250 260 270 GTAGCCATGACTGCACCACTAAGTGGTATG 270 GTAGCCATGACTGCACCACTAAGTGGTATG 270 GTAGCCATGACTGCACCACTAAGTGGTATG 270
- Majority	
Majority	TCAT GGT CTGCCT CAT CTTTTT GT A CAGCT
Ark/Ark-DPI p8/91 inoculum B-4-10 Transmission 3 B-21-12 Transmission 10	TCAT GGT CTGCCT CAT CTTTTT GTA CAGCT 300 TCAT GGT CTGCCT CAT CTTTTT GTA CAGCT 300 TCAT GGT CTGCCT CAT CTTTTT GTA CAGCT 300

- Majority	
Majority	CACTGTAATTTTACTTCTTATATAGTGTTT
Ark/Ark-DPI p8/91 inoculum B-4-10 Transmission 3 B-21-12 Transmission 10	310 320 330 CACTGTAATTTTACTTCTTATATAGTGTTT 330 CACTGTAATTTTACTTCTTATATAGTGTTT 330 CACTGTAATTTTACTTCTTATATAGTGTTT 330
- Majority	
Majority	GTTA CACATT GTTTTA AGA GCGGAT CTA AT
Ark/Ark-DPI p8/91 inoculum B-4-10 Transmission 3 B-21-12 Transmission 10	340 350 360 GTTA CACATT GTTTTA AGA GCGGAT CTA AT 360 GTTA CACATT GTTTTA AGA GCGGAT CTA AT 360 GTTA CACATT GTTTTA AGA GCGGAT CTA AT 360
- Majority	
Majority	AGTT GTCCTTTGA CAGGTCTTATTCCAAGC
Ark/Ark-DPI p8/91 inoculum B-4-10 Transmission 3 B-21-12 Transmission 10	370 390 390 AGTTGTCCTTTGACAGGTCTTATTCCAAGC 390 AGTTGTCCTTTGACAGGTCTTATTCCAAGC 390 AGTTGTCCTTTGACAGGTCTTATTCCAAGC 390
- Majority	
Majority	GGTTATATTCGTATTGCTGCTATGAAACAT
Ark/Ark-DPI p8/91 inoculum B-4-10 Transmission 3 B-21-12 Transmission 10	400 420 GGTTATATTCGTATTGCTGCTATGAAACAT 420 GGTTATATTCGTATTGCTGCTATGAAACAT 420 GGTTATATTCGTATTGCTGCTATGAAACAT 420
- Majority	
Majority	GGAAGTGCTACGCCTGGTCACTTATTTTAT
Ark/Ark-DPI p8/91 inoculum B-4-10 Transmission 3 B-21-12 Transmission 10	430 440 450 GGAAGTGCTACGCCTGGTCACTTATTTTAT 450 GGAAGTGCTACGCCTGGTCACTTATTTTAT 450 GGAAGTGCTACGCCTGGTCACTTATTTTAT 450
Majority	AACTTAACAGTTTCTGTGACTAAATATCCT 460 470 480
Ark/Ark-DPI p8/91 inoculum B-4-10 Transmission 3 B-21-12 Transmission 10	AACTTAACAGTTTCTGTGACTAAATATCCT 480 AACTTAACAGTTTCTGTGACTAAATATCCT 480 AACTTAACAGTTTCTGTGACTAAATATCCT 480
- Majority	
Majority	AAGTTTAGATCGCTACAATGTGTTAATAAT
Ark/Ark-DPI p8/91 inoculum B-4-10 Transmission 3 B-21-12 Transmission 10	490 500 510 AAGTTTAGATCGCTACAATGTGTTAATAAT 510 AAGTTTAGATCGCTACAATGTGTTAATAAT 510 AAGTTTAGATCGCTACAATGTGTTAATAAT 510
- Majority	
Majority	CATACTTCTGTATATTTAAATGGTGACCTT
Ark/Ark-DPI p8/91 inoculum B-4-10 Transmission 3 B-21-12 Transmission 10	520 530 540 CATACTTCTGTATATTTAAATGGTGACCTT 540 CATACTTCTGTATATTTAAATGGTGACCTT 540 CATACTTCTGTATATTTAAATGGTGACCTT 540
- Majority	
Majority	GTTTTCACATCTAACTATACTGAAGATGTT
Ark/Ark-DPI p8/91 inoculum B-4-10 Transmission 3 B-21-12 Transmission 10	550 560 570 GTTTTCACATCTAACTATACTGAAGATGTT 570 GTTTTCACATCTAACTATACTGAAGATGTT 570 GTTTTCACATCTAACTATACTGAAGATGTT 570
- Majority	
Majority	GTAGCTGCAGGTGTCCATTTTAAAAGTGGT 580 590 600
Ark/Ark-DPI p8/91 inoculum B-4-10 Transmission 3 B-21-12 Transmission 10	GTAGCTGCAGGTGTCCATTTTAAAAGTGGT 600 GTAGCTGCAGGTGTCCATTTTAAAAGTGGT 600 GTAGCTGCAGGTGTCCATTTTAAAAGTGGT 600

Majority	GGACCTATAACTTATAAAGTTATGAGAGAG 610 620 630
Ark/Ark-DPI p8/91 inoculum B-4-10 Transmission 3 B-21-12 Transmission 10	GGACCTATAÁCTTATAAAGÍTATGAGAGAG 630 GGACCTATAACTTATAAAGTTATGAGAGAG 630 GGACCTATAACTTATAAAGTTATGAGAGAG 630
- Majority	
Majority	GTTAAAGCCTTGGCTTATTTTGTCAATGGT 640 650 660
Ark/Ark-DPI p8/91 inoculum B-4-10 Transmission 3 B-21-12 Transmission 10	GTTAAAGCCTTGGCTTATTTTGTCAATGGT 660 GTTAAAGCCTTGGCTTATTTTGTCAATGGT 660 GTTAAAGCCTTGGCTTATTTTGTCAATGGT 660
- Majority	
Majority	ACTGCACATGATGTCATTCTATGTGATGAC 670 680 690
Ark/Ark-DPI p8/91 inoculum B-4-10 Transmission 3 B-21-12 Transmission 10	ACTGCACATGATGTCATTCTATGTGATGAC 690 ACTGCACATGATGTCATTCTATGTGATGAC 690 ACTGCACATGATGTCATTCTATGTGATGAC 690
- Majority	
Majority	ACACCTAGAGGTTTGTTAGCATGCCAATAT 700 710 720
Ark/Ark-DPI p8/91 inoculum B-4-10 Transmission 3 B-21-12 Transmission 10	ACACCTA GAGGTTTGTTAGCATGCCAATAT 720 ACACCTA GAGGTTTGTTAGCATGCCAATAT 720 ACACCTA GAGGTTTGTTAGCATGCCAATAT 720
- Majority	
Majority	AATA CTGGCA ATTTTT CAGAT GCTTCTAT
Ark/Ark-DPI p8/91 inoculum B-4-10 Transmission 3 B-21-12 Transmission 10	730 740 750 AATACTGGCAATTTTTCAGATGGCTTCTAT 750 AATACTGGCAATTTTTCAGATGGCTTCTAT 750 AATACTGGCAATTTTTCAGATGGCTTCTAT 750
Majority	GGACCTATAACTTATAAAGTTATGA GAGAG
Ark/Ark-DPI p8/91 inoculum B-4-10 Transmission 3 B-21-12 Transmission 10	610 620 630 GGACCTATAACTTATAAAGTTATGAGAGAG 630 GGACCTATAACTTATAAAGTTATGAGAGAG 630 GGACCTATAACTTATAAAGTTATGAGAGAG 630
- Majority	
Majority	GTTAAAGCCTTGGCTTATTTTGTCAATGGT
Ark/Ark-DPI p8/91 inoculum B-4-10 Transmission 3 B-21-12 Transmission 10	640 650 660 GTTAAAGCCTTGGCTTATTTTGTCAATGGT 660 GTTAAAGCCTTGGCTTATTTTGTCAATGGT 660 GTTAAAGCCTTGGCTTATTTTGTCAATGGT 660
- Majority	
Majority	ACTGCACATGATGTCATTCTATGTGATGAC 670 680 690
Ark/Ark-DPI p8/91 inoculum B-4-10 Transmission 3 B-21-12 Transmission 10	ACTGCACATGATGTCATTCTATGTGATGAC 690 ACTGCACATGATGTCATTCTATGTGATGAC 690 ACTGCACATGATGTCATTCTATGTGATGAC 690
- Majority	
Majority	ACACCTAGAGGTTTGTTAGCATGCCAATAT 700 710 720
Ark/Ark-DPI p8/91 inoculum B-4-10 Transmission 3 B-21-12 Transmission 10	ACACCTA GAGGTTTGTTAGCATGCCAATAT 720 ACACCTA GAGGTTTGTTAGCATGCCAATAT 720 ACACCTA GAGGTTTGTTAGCATGCCAATAT 720
- Majority	
Majority	AATACTGGCAATTTTTCAGATGGCTTCTAT
Ark/Ark-DPI p8/91 inoculum B-4-10 Transmission 3 B-21-12 Transmission 10	AATACTGGCAATTTTTCAGATGGCTTCTAT 750 AATACTGGCAATTTTTCAGATGGCTTCTAT 750 AATACTGGCAATTTTTCAGATGGCTTCTAT 750

### ### ### ### ### ### ### ### ### ##	Majority	CAGA CACAAA CAGCTCAGA GT GGTT ATT AT
Majority	B-4-10 Transmission 3	CAGA CACAAA CAGCTCAGA GTGGTTATTAT 930 CAGA CACAAA CAGCTCAGA GTGGTTATTAT 930
Majority	- Majority	
S40 S50 S50 S50		AATT TTA ATT TTT CAT TTC TGA GT A GT T T T
B-4-10 Transmission 3	,,	
Majority	B-4-10 Transmission 3	AATTTTAATTTTTCATTTCTGAGTAGTTTT 960
Ark/Ark-DPI p8/91 inoculum B4-10 Transmission 3 B-21-12 Transmission 10 - Majority Majority Majority Majority TCTTACCATCCACGTTGTAGTTTTAGACCT 1000 1010 1020 B-4-10 Transmission 3 B-21-12 Transmission 10 - Majority Majority Majority TCTTACCATCCACGTTGTAGTTTTAGACCT 1000 1010 1020 B-4-10 Transmission 3 B-21-12 Transmission 10 - Majority Majority Majority Majority Majority GAAACCCTTAATGGTTTGTGGTTTAATTCC 1020 Ark/Ark-DPI p8/91 inoculum B-4-10 Transmission 10 Majority Majority CAGACACAAACAGCTCAGAGTGGTTATTTATTC 1050 GAAACCCTTAATGGTTTGTGGTTTAATTCC 1050 GAAACCCTTAATGGTTTGTGGTTTAATTCC 1050 GAAACCCTTAATGGTTTGTGGTTTAATTCC 1050 GAAACCCTTAATGGTTTGTGGTTTAATTCC 1050 GAAACCCTTAATGGTTTGTGGTTATTAT 300 Ark/Ark-DPI p8/91 inoculum B-4-10 Transmission 3 B-21-12 Transmission 10 - Majority Majority AATTTTAATTTTCATTTCTGAGTAGTTTTT 900 Ark/Ark-DPI p8/91 inoculum B-4-10 Transmission 10 - Majority Majority AATTTTAATTTTTCATTTCTGAGTAGTTTTT 900 Ark/Ark-DPI p8/91 inoculum B-4-10 Transmission 3 B-21-12 Transmission 10 - Majority Majority AATTTTAATTTTTCATTTCTGAGTAGTTTTT 900 Ark/Ark-DPI p8/91 inoculum B-4-10 Transmission 3 B-21-12 Transmission 3 B-21-12 Transmission 10 - Majority Majority AATTTTAATTTTTCATTTCTGAGTAGTTTTT 900 Ark/Ark-DPI p8/91 inoculum B-4-10 Transmission 3 B-21-12 Transmission 10 - Majority Majority ATTTAATGGGAAAGTAATTATATGGAGAGGGAGGAGGAGG	- Majority	
Ark/Ark-DPI p8/91 inoculum	Majority	
Majority TCTTACCATCCACGTT GTA GTTTTA GACCT 1020 Ark/Ark-DPI p8/91 inoculum B-4-10 Transmission 3 B-21-12 Transmission 10 TCTTACCATCCACGTT GTA GTTTTA GACCT 1020 - Majority TCTTACCATCCACGTT GTA GTTTTA GACCT 1020 - Majority GAAACCCTTAATGGTTTGT GGTTTAATTCC 1050 1030 1040 1050 - Ark/Ark-DPI p8/91 inoculum B-4-10 Transmission 3 GAAACCCTTAATGGTTTGT GGTTTAATTCC 1050 105-1050 105-1050 1050 1050 1050 1	B-4-10 Transmission 3	GTTTATAGGGAAAGTAATTATATGTATGGA 990 GTTTATAGGGAAAGTAATTATATGTATGGA 990
1000	- Majority	
Ark/Ark-DPI p8/91 inoculum	Majority	
B-4-10 Transmission 10 TCTT ACCATC CACGTT GTA GTTTTA GACCT 1020	Ark/Ark-DPI p8/91 inoculum	
Majority GAAA CCCTTA ATGGTTTGT GGTTTA ATTCC 1050 Ark/Ark-DPI p8/91 inoculum B-4-10 Transmission 3 B-21-12 Transmission 10 GAAA CCCTTA ATGGTTTGT GGTTTA ATTCC 1050 GAAA CACAAA CAGCTCAGA GTGGTTATTAT 930 GAACAAAA CAGCTCAGA GTGGTTATTAT 930 GAGA CACAAA CAGCTCAGA GTAGTTTT 960 GAGA GTAGTTTT ATGGA GTAGTTT 960 GAGA GTAGTTTT ATGGA GTAG	B-4-10 Transmission 3	TCTTACCATCCACGTTGTAGTTTTAGACCT 1020
1030	- Majority	
Ark/Ark-DPI p8/91 inoculum B-4-10 Transmission 3 B-21-12 Transmission 10 Majority CAGA CACAAA CAGCTC AGA GT GGT TATAT T T	Majority	
B-4-10 Transmission 3 GAAA CCCTTA ATGGTTTGT GGTTTA ATTCC		GAAACCCTTAATGGTTTGTGGTTTAATTCC 1050
910 920 930		GAAACCCTTAATGGTTTGTGGTTTAATTCC 1050
Ark/Ark-DPI p8/91 inoculum CAGA CACAAA CAGCTCAGA GT GGTTATTAT 930 B-4-10 Transmission 3 CAGA CACAAA CAGCTCAGA GT GGTTATTAT 930 B-21-12 Transmission 10 CAGA CACAAA CAGCTCAGA GT GGTTATTAT 930 - Majority AATTTTAATTTTTCATTTCTGAGTAGTTTT 940 950 960 Ark/Ark-DPI p8/91 inoculum AATTTTAATTTTCATTTCTGAGTAGTTTT 960 B-21-12 Transmission 3 AATTTTAATTTTTCATTTCTGAGTAGTTTT 960 B-21-12 Transmission 10 AATTTTAATTTTCATTTCTGAGTAGTTTT 960 - Majority GTTTATAGGGAAAGTAATTATATGTATGGA 970 980 990 Ark/Ark-DPI p8/91 inoculum GTTTATAGGGAAAGTAATTATATGTATGGA 990 990 B-4-10 Transmission 3 GTTTATAGGGAAAGTAATTATATGTATGGA 990 B-21-12 Transmission 10 GTTTATAGGGAAAGTAATTATATGTATGGA 990 - Majority TCTTACCATCCACGTTGTAGTTTTAGACCT TCTTACCATCCACGTTGTAGTTTTAGACCT	Majority	
Majority AATTTTAATTTTCATTTCTGAGTAGTTTT 940 950 960 Ark/Ark-DPI p8/91 inoculum AATTTTAATTTTCATTTCTGAGTAGTTTT 960 B-4-10 Transmission 3 AATTTTAATTTTCATTTCTGAGTAGTTTT 960 - Majority AATTTTAATTTTCATTTCTGAGTAGTTTT 960 - Majority GTTTATAGGGAAAGTAATTATATGTATGGA 970 980 990 Ark/Ark-DPI p8/91 inoculum GTTTATAGGGAAAGTAATTATATGTATGGA 990 B-4-10 Transmission 3 GTTTATAGGGAAAGTAATTATATGTATGGA 990 B-21-12 Transmission 10 GTTTATAGGGAAAGTAATTATATGTATGGA 990 - Majority TCTTACCATCCACGTTGTAGTTTTAGACCT TTTTAGACCTTCACGTTGTAGTTTTAGACCT TTTTTTTTTTTTTTTTTTTTTTTTTTTTTTTTTTTT	B-4-10 Transmission 3	CAGA CACAAA CAGCTCAGA GTGGTTATTAT 930 CAGA CACAAA CAGCTCAGA GTGGTTATTAT 930
Majority AATTTTAATTTTCATTTCTGAGTAGTTTT 940 950 960 Ark/Ark-DPI p8/91 inoculum AATTTTAATTTTCATTTCTGAGTAGTTTT 960 B-4-10 Transmission 3 AATTTTAATTTTCATTTCTGAGTAGTTTT 960 - Majority AATTTTAATTTTCATTTCTGAGTAGTTTT 960 - Majority GTTTATAGGGAAAGTAATTATATGTATGGA 970 980 990 Ark/Ark-DPI p8/91 inoculum GTTTATAGGGAAAGTAATTATATGTATGGA 990 B-4-10 Transmission 3 GTTTATAGGGAAAGTAATTATATGTATGGA 990 B-21-12 Transmission 10 GTTTATAGGGAAAGTAATTATATGTATGGA 990 - Majority TCTTACCATCCACGTTGTAGTTTTAGACCT TTTTAGACCTTCACGTTGTAGTTTTAGACCT TTTTTTTTTTTTTTTTTTTTTTTTTTTTTTTTTTTT	- Majority	
940 950 960		AATT TTA ATT TTT CAT TTC TGA GT A GT T TT
B-4-10 Transmission 3	,	
- Majority Majority GTTTATAGGGAAAGTAATTATATGTATGGA 970 980 990 Ark/Ark-DPI p8/91 inoculum B-4-10 Transmission 3 B-21-12 Transmission 10 - Majority Majority GTTTATAGGGAAAGTAATTATATGTATGGA 990 GTTTATAGGGAAAGTAATTATATGTATGGA 990 TCTTACCATCCACGTTGTAGTTTTAGACCT	Ark/Ark-DPI p8/91 inoculum B-4-10 Transmission 3	
Majority GTTTATAGGGAAAGTAATTATATGTATGGA	B-21-12 Transmission 10	AATTTTAATTTTCATTTCTGAGTAGTTTT 960
970 980 990	- Majority	
Ark/Ark-DPI p8/91 inoculum B-4-10 Transmission 3 B-21-12 Transmission 10 - Majority Ark/Ark-DPI p8/91 inoculum GTTTATA GGGAAA GTAATTATATGTATGGA 990 GTTTATA GGGAAA GTAATTATATGTATGGA 990 - Majority TCTTACCATCCACGTT GTAGTTTTA GACCT	Majority	
B-4-10 Transmission 3 B-21-12 Transmission 10 GTTTATA GGG AAA GTA ATTATAT GTAT GGA 990 GTTTATA GGG AAA GTA ATTATAT GTAT GGA 990 - Majority Majority TCTTACCATCCACGTT GTA GTTTTA GACCT	Ark/Ark-DPI p8/91 inoculum	
Majority <u>TCTT ACCAT CCACGTT GT A GT T T T A GACCT</u>	B-4-10 Transmission 3	
Majority <u>TCTT ACCAT CCACGTT GT A GT T T T A GACCT</u>	- Majority	
· · · · · · · · · · · · · · · · · · ·		TCTTACCATCCACGTTGTAGTTTTAGACCT
	,,	
Ark/Ark-DPI p8/91 inoculum TCTT ACCATC CACGTT GTA GTTTTA GACCT 1020 B-4-10 Transmission 3 TCTT ACCATC CACGTT GTA GTTTTA GACCT 1020 B-21-12 Transmission 10 TCTT ACCATC CACGTT GTA GTTTTA GACCT 1020	B-4-10 Transmission 3	TCTTACCATCCACGTTGTAGTTTTAGACCT 1020
- Majority	- Majority	
Majority <u>GAAACCCTTAATGGTTTGTGGTTTAATTCC</u>	Majority	GA A A CCCTT A ATGGTT TGT GGT TTA ATT CC
1030 1040 1050		annoco I I na I da I I I na I I da I I na I I da I I na I I da I I na I da I I na I I da I I na I da I na I n
	Adv/Adv DDI p0/01 inner tree	1030 1040 1050
B-4-10 Transmission 3 GAAA CCCTTA ATGGTTTGT GGTTTA ATT CC 1050 B-21-12 Transmission 10 GAAA CCCTTA ATGGTTTGT GGTTTA ATT CC 1050		1030 1040 1050 GAAACCCTTAATGGTTTGTGGTTTAATTCC 1050 GAAACCCTTAATGGTTTGTGGTTTAATTCC 1050

Majority	CTTTCTGTTTCATTAACATACGGTCCCATT
	1060 1070 1080
Ark/Ark-DPI p8/91 inoculum	CTTTCTGTTTCATTAACATACGGTCCCATT 1080 CTTTCTGTTTCATTAACATACGGTCCCATT 1080
B-4-10 Transmission 3 B-21-12 Transmission 10	CTTTCTGTTTCATTAACATACGGTCCCATT 1080 CTTTCTGTTTCATTAACATACGGTCCCATT 1080
- Majority	
Majority	CAAGGTGGTTGTAAGCAATCTGTATTTAAT
Wajority	
Ark/Ark-DPI p8/91 inoculum	1090 1100 1110 CAAGGTGGTTGTAAGCAATCTGTATTTAAT 1110
B-4-10 Transmission 3	CAAGGTGGTTGTAAGCAATCTGTATTTAAT 1110 CAAGGTGGTTGTAAGCAATCTGTATTTAAT 1110
B-21-12 Transmission 10	CAAGGTGGTTGTAAGCAATCTGTATTTAAT 1110
- Majority	
Majority	GGT A AAGCAACTT GTT GTT AT GCTT ATT CA
	1120 1130 1140
Ark/Ark-DPI p8/91 inoculum	GGT A A A G C A A C T T G T T A T G C T A T T C A 1140
B-4-10 Transmission 3 B-21-12 Transmission 10	GGTAAAGCAACTTGTTGTTATGCTTATTCA 1140 GGTAAAGCAACTTGTTGTTATGCTTATTCA 1140
D 21-12 Hallomosion To	adi AAAdaAA OTT di TATTA OTT ATT OA TITO
- Majority	
Majority	TACGGAGGACCTCGTGCTTGTAAAGGTGTC
	1150 1160 1170
Ark/Ark-DPI p8/91 inoculum B-4-10 Transmission 3	TACGGAGGACCTCGTGCTTGTAAAGGTGTC 1170 TACGGAGGACCTCGTGCTTGTAAAGGTGTC 1170
B-21-12 Transmission 10	TACGGAGGACCTCGTGCTTGTAAAGGTGTC 1170
- Majority	
Majority	TATAGAGGTGAGCTAACACAGCATTTTGAA
	1180 1190 1200
Ark/Ark-DPI p8/91 inoculum	TATAGAGGTGAGCTAACACAGCATTTTGAA 1200
B-4-10 Transmission 3 B-21-12 Transmission 10	TATA GAGGTGAGCTAA CACAGCATTTTGAA 1200 TATA GAGGTGAGCTAA CACAGCATTTTGAA 1200
D-21-12 Hansinission to	TATAGAGGTAAGAGATTTTGAA 1200
Majority	TGTGGTTTGTTAGTTTATGTTACTAAGAGC
,,	1210 1220 1230
Ark/Ark-DPI p8/91 inoculum	TGTGGTTTGTTAGTTTATGTTACTAAGAGĆ 1230 TGTGGTTTGTTAGTTTATGTTACTAAGAGC 1230
B-4-10 Transmission 3 B-21-12 Transmission 10	TGTGGTTTGTTAGTTTATGTTACTAAGAGC 1230 TGTGGTTTGTTAGTTTATGTTACTAAGAGC 1230
- Majority	
Majority	GATGGCTCCCGTATACAAACTGCAACACAA
Ark/Ark-DPI p8/91 inoculum	1240 1250 1260 GATGGCTCCCGTATACAAACTGCAACACAA 1260
B-4-10 Transmission 3	GATGGCTCCCGTATACAAACTGCAACACAA 1260
B-21-12 Transmission 10	GATGGCTCCCGTATACAAACTGCAACACAA 1260
- Majority	
Majority	CCACCTGTATTAACCCAAAATTTTTATAAT
	1270 1280 1290
Ark/Ark-DPI p8/91 inoculum B-4-10 Transmission 3	CCACCTGTATTAACCCAAAATTTTTATAAT 1290 CCACCTGTATTAACCCAAAATTTTTATAAT 1290
B-21-12 Transmission 10	CCACCTGTATTAACCCAAAATTTTTATAAT 1290
Majority	
- Majority	
Majority	AACATCACTTTAGGTAAGTGTGTTGATTAT 1300 1310 1320
Ark/Ark-DPI p8/91 inoculum	
B-4-10 Transmission 3 B-21-12 Transmission 10	AACATCACTTTAGGTAAGTGTGTTGATTAT 1320 AACATCACTTTAGGTAAGTGTGTTGATTAT 1320 AACATCACTTTAGGTAAGTGTGTTGATTAT 1320
2 2 12 Transmission 10	
- Majority	
Majority	AATGTTT ATGGT A GAA CTGGA CAAGGTTTT
	1330 1340 1350
Ark/Ark-DPI p8/91 inoculum B-4-10 Transmission 3	AATGTTTATĠGTAGAACTGĠACAAGGTTTŤ 1350 AATGTTTATGGTAGAACTGGACAAGGTTTT 1350
B-21-12 Transmission 10	AATGTTTATGGTAGAACTGGACAAGGTTTT 1350

Majority	ATTACTAATGTAACTGATTTAGCTACTTCT
Ark/Ark-DPI p8/91 inoculum B-4-10 Transmission 3 B-21-12 Transmission 10	1360 1370 1380 ATTACTAATGTAACTGATTTAGCTACTTCT 1380 ATTACTAATGTAACTGATTTAGCTACTTCT 1380 ATTACTAATGTAACTGATTTAGCTACTTCT 1380
- Majority	
Majority	CATAATTACTTAGCGGATGGAGGATTAGCT
Ark/Ark-DPI p8/91 inoculum B-4-10 Transmission 3 B-21-12 Transmission 10	1390 1400 1410 CATAATTACTTAGCGGATGGAGGATTAGCT 1410 CATAATTACTTAGCGGATGGAGGATTAGCT 1410 CATAATTACTTAGCGGATGGAGGATTAGCT 1410
- Majority	
Majority	ATTTTAGATA CATCTGGTGCCATAGACATC
Ark/Ark-DPI p8/91 inoculum B-4-10 Transmission 3 B-21-12 Transmission 10	ATTTTAGATA CATCTGGTGCCATAGACATC 1440 ATTTTAGATA CATCTGGTGCCATAGACATC 1440 ATTTTAGATA CATCTGGTGCCATAGACATC 1440 ATTTTAGATA CATCTGGTGCCATAGACATC 1440
- Majority	
Majority	TTCGTTGTACAAGGTGAATATGGCCCTAAC 1450 1460 1470
Ark/Ark-DPI p8/91 inoculum B-4-10 Transmission 3 B-21-12 Transmission 10	TTCGTTGTACAAGGTGAATATGGCCCTAAC 1470 TTCGTTGTACAAGGTGAATATGGCCCTAAC 1470 TTCGTTGTACAAGGTGAATATGGCCCTAAC 1470
- Majority	
Majority	TACTATAAGGTTAATCTATGTGAAGATGTT 1480 1490 1500
Ark/Ark-DPI p8/91 inoculum B-4-10 Transmission 3 B-21-12 Transmission 10	TACTATAAGGTTAATCTATGTGAAGATGTT 1500 TACTATAAGGTTAATCTATGTGAAGATGTT 1500 TACTATAAGGTTAATCTATGTGAAGATGTT 1500 TACTATAAGGTTAATCTATGTGAAGATGTT 1500
Majority	AACCAACAGTTTGTAGTTTCTGGTGGTAAA
Ark/Ark-DPI p8/91 inoculum B-4-10 Transmission 3 B-21-12 Transmission 10	1510 1520 1530 AACCAACAGTTTGTAGTTTCTGGTGGTAAA 1530 AACCAACAGTTTGTAGTTCTGGTGGTAAA 1530 AACCAACAGTTTGTAGTTTCTGGTGGTAAA 1530
- Majority	
Majority	TTAGTAGGTATTCTCACTTCACGTAATGAA
Ark/Ark-DPI p8/91 inoculum B-4-10 Transmission 3 B-21-12 Transmission 10	1540 1550 1560 TTAGTAGGTATTCTCACTTCACGTAATGAA 1560 TTAGTAGGTATTCTCACTTCACGTAATGAA 1560 TTAGTAGGTATTCTCACTTCACGTAATGAA 1560
- Majority	
Majority	ACTGGTTCTCAGCCTCTTGAAAACCAGTTT 1570 1580 1590
Ark/Ark-DPI p8/91 inoculum B-4-10 Transmission 3 B-21-12 Transmission 10	ACTGGTTCTCAGCCTCTTGAAAACCAGTTT 1590 ACTGGTTCTCAGCCTCTTGAAAACCAGTTT 1590 ACTGGTTCTCAGCCTCTTGAAAACCAGTTT 1590
- Majority	
Majority	TACATTAAGATCACTAATGGAACACATC 1600 1610
Ark/Ark-DPI p8/91 inoculum B-4-10 Transmission 3 B-21-12 Transmission 10	TACATTA AGATCA CTA ATGGA A CACATC 1618 TACATTA AGA TCA CTA ATGGA A CACATC 1618 TACATTA AGA TCA CTA ATGGA A CACATC 1618

Figure 5.5. Alignment of S1 of Arkansas DPI: inoculum, virus isolated from B-4 (Transmission 3), and B-21 (Transmission 10).

CHAPTER 6

CONCLUSIONS

Exoribonuclease Active site is conserved in Infectious Bronchitis Virus

Recently, an exoribonuclease domain was identified in the SARS-CoV nonstructural protein 14, which indicates some level of proof reading capabilities, may be present in CoV. We examined nsp 14 in gammacoronavirues and found that the DEDD active site of the predicted exoribonuclease domain and the MTase domains are present in gammacoronaviruses specifically IBV. These data suggest that IBV may have proofreading capabilities similar to other CoVs (3). This information is important for understanding how CoVs can replicate below their error threshold while still maintaining a large genome and it could aid in the development of a reversion-resistant live attenuated vaccines.

Feline Infectious Peritonitis Virus does not adapt to cell culture in the spike gene

It is not clear if mutations occur in FECV, causing FIPV, or if in fact, they are separate circulating viruses. In this study, we examined the capacity of FIPV to change following passage in cell culture. We found little or no changes occur across the full-length of the genome as well as biologically (growth kinetics) in FCoV following passage in canine A-72 cells. These data indicate that FIPV is relatively stable. In addition, because different selection pressures occur *in vitro* and *in vivo*, it is possible that mutations in FECV could occur giving rise to FIPV during a natural infection.

Infectious Bronchitis Virus Transmission Dynamics

The IBV strain Ark/Ark-DPI p8/91 was naturally transmitted in chickens ten times. During this transmission study, tracheal and choanal cleft swabs were taken for virus isolation, and no statistical difference was found in the detection of the virus or the amount of viral genome present at the same time point from the same bird. Thus, choanal cleft swabbing can be used for future temporal IBV studies to prevent damage to the epithelial cells in the trachea, which is the primary replication site of IBV. For the transmission study, the average maximum viral load peaked at 6.5 days with an average genome copy number was 1 X 10^{5.379} per sample. The virus was more rapidly transmitted among chicks after the third transmission indicating selection/adaptation had occurred. However, the virus was also cleared faster by the birds in the later transmission events. As the experiment progressed, the age of the birds increased and thus the maturity of the immune system, which could possibly account for the decrease observed for the infectious period. It is not clear if the age of the birds would affect the rate of transmission. However, age should be considered when estimating or calculating values for R0. No nucleotide changes were observed in the S1 consensus sequence of IBV isolated from the inoculum, transmission 3, and transmission 10. These data indicate that selection pressures are likely acting on other areas of the viral genome. Understanding transmission dynamics of IBV will aid in the design of future control strategies for this economically important virus.